13. Kawate K, Yajima H, Ohgushi H, Kotobuki N, Sugimoto K, Ohmura T, Kobata Y, Shigematsu K, Kawamura K, Tamai K, Takakura Y. Tissue-engineered approach for the treatment of steroid-induced osteonecrosis of the femoral head: transplantation of autologous mesenchymal stem cells cultured with beta-tricalcium phosphate ceramics and free vascularized fibula. Artif Organs. **30,** 960, 2006.
14. Dezawa M, Ishikawa H, Itokazu Y, Yoshihara T, Hoshino M, Takeda S, Ide C, Nabeshima Y. Bone marrow stromal cells generate muscle cells and repair muscle degeneration. Science. **309,** 314, 2005.
15. Dezawa M, Kanno H, Hoshino M, Cho H, Matsumoto N, Itokazu Y, Tajima N, Yamada H, Sawada H, Ishikawa H, Mimura T, Kitada M, Suzuki Y, Ide C. Specific induction of neuronal cells from bone marrow stromal cells and application for autologous transplantation. J Clin Invest. **113,** 1701, 2004.
16. Mimura T, Dezawa M, Kanno H, Yamamoto I. Behavioral and histological evaluation of a focal cerebral infarction rat model transplanted with neurons induced from bone marrow stromal cells. J Neuropathol Exp Neurol. **64,** 1108, 2005.
17. Akerud P, Alberch J, Eketjall S, Wagner J, Arenas E. Differential effects of glial cell line-derived neurotrophic factor and neurturin on developing and adult substantia nigra dopaminergic neurons. J Neurochem. **73,** 70, 1999.
18. Mangi AA, Noiseux N, Kong D, He H, Rezvani M, Ingwall JS, Dzau VJ. Mesenchymal stem cells modified with Akt prevent remodeling and restore performance of infarcted hearts. Nat Med. **9,** 1195, 2003.
19. Yokoo T, Ohashi T, Shen JS, Sakurai K, Miyazaki Y, Utsunomiya Y, Takahashi M, Terada Y, Eto Y, Kawamura T, Osumi N, Hosoya T. Human mesenchymal stem cells in rodent whole-embryo culture are reprogrammed to contribute to kidney tissues. Proc Natl Acad Sci U S A. **102,** 3296, 2005.
20. Okazaki A, Jo J, Tabata Y. A reverse transfection technology to genetically engineer adult stem cells. Tissue Eng. **13,** 245, 2007.
21. Hermanson GT. Bioconjugate Techniques, San Diego, CA: Academic Press; 1996.
22. Yamamoto N, Yamamoto S, Inagaki F, Kawaichi M, Fukamizu A, Kishi N, Matsuno K, Nakamura K, Weinmaster G, Okano H, Nakafuku M. Role of Deltex-1 as a transcriptional regulator downstream of the Notch receptor. J Biol Chem. **276,** 45031, 2001.
23. Dezawa M, Takahashi I, Esaki M, Takano M, Sawada H. Sciatic nerve regeneration in rats induced by transplantation of in vitro differentiated bone-marrow stromal cells. The European journal of neuroscience. **14,** 1771, 2001.
24. Habeeb AF. Determination of free amino groups in proteins by trinitrobenzenesulfonic acid. Anal Biochem. **14,** 328, 1966.
25. Nagano Y, Yamashita H, Takahashi T, Kishida S, Nakamura T, Iseki E, Hattori N, Mizuno Y, Kikuchi A, Matsumoto M. Siah-1 facilitates ubiquitination and degradation of synphilin-1. J Biol Chem. **278,** 51504, 2003.
26. Kopen GC, Prockop DJ, Phinney DG. Marrow stromal cells migrate throughout forebrain and cerebellum, and they differentiate into astrocytes after injection into neonatal mouse brains. Proc Natl Acad Sci U S A. **96,** 10711, 1999.
27. Shimizu S, Kitada M, Ishikawa H, Itokazu Y, Wakao S, Dezawa M. Peripheral nerve regeneration by the in vitro differentiated-human bone marrow stromal cells with Schwann cell property. Biochem Biophys Res Commun. **359,** 915, 2007.
28. Kawasaki H, Mizuseki K, Nishikawa S, Kaneko S, Kuwana Y, Nakanishi S, Nishikawa SI, Sasai Y. Induction of midbrain dopaminergic neurons from ES cells by stromal cell-derived inducing activity. Neuron. **28,** 31, 2000.

Address reprint requests to:
Mari Dezawa, M.D., Ph.D.
Department of Stem Cell Biology and Histology
Tohoku University Graduate School of Medicine
2-1 Seiryo-machi, Aoba-ku, Sendai 980-8575
Japan

E-mail: mdezawa@m.tains.tohoku.ac.jp

Received: August 8, 2008
Accepted: October 15, 2008
Online Publication Date: January 16, 2009

The American Journal of Pathology, Vol. 172, No. 3, March 2008

DOI: 10.2353/ajpath.2008.061249

Epithelial and Mesenchymal Cell Biology

Controlled Delivery of T-box21 Small Interfering RNA Ameliorates Autoimmune Alopecia (Alopecia Areata) in a C3H/HeJ Mouse Model

Motonobu Nakamura,*† Jun-ichiro Jo,‡ Yasuhiko Tabata,‡ and Osamu Ishikawa*

From the Department of Dermatology, Gunma University, Maebashi; the Department of Dermatology,† Kyoto University, Kyoto; and the Department of Biomaterials,‡ Field of Tissue Engineering, Institute for Frontier Medical Sciences, Kyoto University, Kyoto, Japan*

Autoimmune alopecia (alopecia areata) is considered to be triggered by a collapse of immune privilege in hair follicles. Here we confirmed that infiltrating CD4 T lymphocytes around hair follicles of patients with alopecia areata were primarily CCR5-positive with few CCR4-positive cells, suggesting a dominant role of Th1 cells in the alopecic lesion. Given this finding, we sought to elucidate the effect of cytokine therapy in C3H/HeJ mice, a mouse model of alopecia areata, by applying recombinant interleukin-4 and neutralizing anti-interferon-γ antibody. We found that local injections of both interleukin-4 and neutralizing anti-interferon-γ antibody effectively treated alopecia in C3H/HeJ mice. Results from immunohistochemistry and semiquantitative reverse transcription-polymerase chain reaction demonstrated that intralesional injection of interleukin-4 suppressed CD8 T cell infiltrates around the hair follicles and repressed enhanced interferon-γ mRNA expression in the affected alopecic skin. Furthermore, Th1 transcription factor T-box21 small interfering RNAs conjugated to cationized gelatin showed mitigating effects on alopecia in C3H/HeJ mice, resulting in the restoration of hair shaft elongation. Taken together, the use of gelatin–small interfering RNA conjugates promises to be a novel, efficient, and safe tool as an alternative gene therapy for the treatment of various human diseases. To our knowledge, this is the first report of effective controlled delivery of small interfering RNA using biodegradable cationized gelatin microspheres in an animal model of disease. ***(Am J Pathol 2008, 172:650–658; DOI: 10.2353/ajpath.2008.061249)***

Alopecia areata is a tissue-restricted autoimmune disease directed at the hair follicle resulting in hair loss.[1,2] It is a common disorder with an estimated prevalence of 1 in 1000 and sometimes extends to the whole scalp area (alopecia totalis). Total loss of scalp and body hair (alopecia universalis) may take place. Patients often feel severe psychological stress from this hair loss; however, conventional therapies such as topical immunotherapy or steroid application often fail to cure the disease.

Since HLA-DR and ICAM1 are ectopically expressed in the outer sheath cells, a collapse of immune privilege is considered to lead to the initiation of alopecia areata. T lymphocytes from the patients could cause alopecia areata, when cultured with hair follicle homogenate along with antigen-presenting cells and injected into the skin explants on severe combined immunodeficiency mice.[3] Purified T cell injection experiments result suggested that both CD4- and CD8-positive T cells have a role in pathogenesis of alopecia areata, CD8-positive cells acting as the main effector cells with the regulatory control by CD4-positive T cells.[4] This study was undertaken to clarify whether Th1 CD4 lymphocytes or Th2 CD4 lymphocytes are dominant in the lesions of patients with alopecia areata and also to elucidate the effect of cytokine therapy applying recombinant interleukin-4 (Il4) and neutralizing anti-interferon-γ (Ifng) antibody into the alopecia areata rodent model C3H/HeJ mice.

Gene therapy is a new therapeutic approach for alopecia areata. Small interfering RNA (siRNA) specifically binds to corresponding mRNA sequence and facilitates its breakage and degradation.[5] Gene therapy using siRNA *in vivo* has been exploited successfully in several mouse disease models; intravenous injections of siRNA limited the rate of metastasis of prostate cancer,[6] and intralesional injections of siRNA decreased the incidence of herpes simplex virus infection.[7] Here we introduced

Supported by Grant-in-Aid 18591233 for Scientific Research from the Ministry of Education, Culture, Sports, Science, and Technology of Japan.

Accepted for publication November 27, 2007.

Address reprint requests to Motonobu Nakamura, Department of Dermatology, Graduate School of Medicine, Kyoto University, 54 Kawahara-cho, Sakyo-ku, Kyoto, 606-8507, Japan. E-mail: motonaka@kuhp.kyoto-u.ac.jp.

another siRNA drug delivery system using cationized gelatin[8] as a new therapeutic approach, targeting T-box21 gene (*Tbx21*) to repress the expression of interferon-γ gene (*Ifng*). *Tbx21* gene was formerly known as *T-bet* gene and plays an important role in control of the *Ifng* gene expression and Th1 cell differentiation and function.[9,10]

Materials and Methods

Patients

Four patients (three males and one female, mean age 29 years) with multiple alopecia areata of 2 to 8 months' duration in active stages were included in this study. Written informed consents were obtained after the aim, nature, and possible consequences of the study were explained. Protocols were approved by the Ethical Committee of Kyoto University. All four patients satisfied the criteria for alopecia areata proposed by American Academy of Dermatology.[11]. None of the patients had any therapy for 60 days before the scalp skin biopsy.

Skin Biopsies

Two skin specimens, 4 mm in diameter and 6 mm in diameter, were obtained from the peripheral region of the alopecic skin of each patient. The former was fixed in formalin and processed for hematoxylin and eosin staining. The latter was snap-frozen in liquid nitrogen and stored at −80°C until use for immunohistochemistry.

Immunohistochemistry

Fluorescence immunohistochemistry was performed on the serial skin cryosections (6 μm) according to an established immunohistochemistry protocol.[12] In brief, cryostat sections (6 μm) were fixed in acetone (10 minutes at −20°C), washed in phosphate-buffered saline (PBS) three times, blocked with 10% goat serum for 20 minutes at room temperature, and incubated overnight at 4°C with mouse anti-human CD4 antibody (1:100, DAKO Cytomation MT310, Kyoto, Japan), mouse anti-human CCR5 antibody (1:100, DAKO Cytomation RB181), and anti-CCR4 antibody (1:100 MAB 1567, R&D Systems, Minneapolis, MN). After further washing with PBS for 5 minutes three times, fluorescein isothiocyanate-labeled goat anti-mouse IgG (1:200, sc-2010, Santa Cruz Biotechnology, Santa Cruz, CA), phycoerythrin-labeled goat anti-mouse IgG (1:200, sc-3738, Santa Cruz Biotechnology), or fluorescein isothiocyanate-labeled goat anti-rat IgG (1:200, sc-2011, Santa Cruz Biotechnology) was applied for 45 minutes at room temperature. After further washing with PBS three times, sections were counterstained with 4′,6-diamino-2-phenylindole. Sections without primary antibody served as negative controls. Mouse CD8 staining was performed using 100X diluted anti-mouse CD8 antibody (sc-18660, Santa Cruz Biotechnology) and LSAB+ System-HRP (DAKO Cytomation, Glostrup, Denmark) according to the manufacturer's instructions. The number of CD8-positive T cells in each hair follicle was counted for 20 hair follicles in four mice before and after Il4 administration.

Animals

Ten-week-old or older female C3H/HeJ mice having an alopecic region on the back in the waxing phase were purchased from SLC company (Hamamatsu, Japan). Mice were maintained at the Institute of Laboratory Animals, Graduate School of Medicine, Kyoto University, and were fed water and mouse chow ad libitum in compliance with protocols established by the Animal Research Committee of Kyoto University. To avoid the possibility of grooming between the mice, mice were put in separate cages. Whole animal care and experimental procedures were approved by the Graduate School of Medicine, Kyoto University. In total, 78 C3H/HeJ mice with alopecic lesions were used in this study: 10 with Il4 injections, 10 with 0.9% sodium chloride injections, 10 with Il4 and Ifng injections, six with anti-Ifng antibody injections, six with rat IgG injections, six with antisense *Tbx21* oligonucleotide injections, six with non-sense oligonucleotide injections, eight with cationized gelatin-conjugated *Tbx21* siRNA injections, eight with naked *Tbx21* siRNA injections, and eight with cationized gelatin-conjugated non-sense siRNA injections.

Semiquantitative Reverse Transcription-PCR (RT-PCR)

RT-PCR was performed on the published protocol. Total RNA from homogenized full-thickness back skin from C3H/HeJ mice was extracted using Qiagen RNeasy Mini Kit (Qiagen, Hilden, Germany) according to the protocol provided by the company. Subsequently, cDNA was synthesized from 1 μg of total RNA using a first-strand cDNA synthesis kit for RT-PCR (AMV) (Boehringer Mannheim, Germany). The reverse-transcribed cDNA was stored at −80°C for further use. Primers used were formerly described[13] and are listed as follows: *Ifng* forward: 5′-AACGCTACACACTGCATCTTGG-3′; *Ifng* reverse: 5′-GACTTCAAAGAGTCTGAGG-3′; *Il12b* forward: 5′-CGTGCTCATGGCTGGTGCAAAG-3′; *Il12b* reverse: 5′-CTTCATCTGCAAGTTCTTGGGC-3′; *Il4* forward: 5′-GAATGTACCAGGAGCCATATC-3′; *Il4* reverse: 5′-CTCAGTACTACGAGTAATCCA-3′; *Actb* forward: 5′-TGTTACCAACTGGGACGACA-3′; *Actb* reverse: 5′-TCTCAGCTGTGGTGGTGAAG-3′. The PCR was run on an Astec Program Temp Control System (Astec, Fukushima, Japan). The reaction consisted of 1 μl of cDNA, 10 μl of 10X PCR buffer, 8 μl of deoxynucleoside-5′-triphosphate mixture (2.5 mmol/L each), 1 μl of forward primer (50 pmol), 1 μl of reverse primer (50 pmol), 0.5 μl of TaKaRa Ex Taq polymerase (Takara, Otsu, Japan), and 78.5 μl of water. Amplification was performed over 32 cycles for *Actb*, 40 cycles for *Ifng*, 40 cycles for *Il12b*, and 45 cycles for *Il4*. Each cycle consisted of the following steps: denaturation at 94°C, annealing at 55°C, and extension at 72°C. The PCR products were analyzed by agarose gel electro-

phoresis. Densitometry was performed by using Epson Color Imaging ES-2200 and National Institutes of Health Image software for assessing staining results.

Application of Il4 and Anti-Ifng Antibody

Recombinant mouse Il4 and rat anti-mouse Ifng neutralizing antibody (MAB485) were purchased from R&D Systems (Minneapolis, MN). Recombinant mouse Ifng was purchased from Pepro Tech (London, UK). Recombinant mouse Il4 was dissolved in 0.9% sodium chloride and injected subcutaneously at a concentration of 0.1 μg/0.2 ml into 10 alopecic lesions every day for 21 days. Sodium chloride, 0.9%, was applied to 10 alopecic lesions as a negative control. Recombinant mouse Ifng was dissolved in 0.9% sodium chloride and injected subcutaneously at a concentration of 0.01 μg/0.1 ml in conjunction with 0.1 μg/0.1 ml recombinant mouse Il4 into 10 alopecic lesions every day for 21 days. The effect was assessed every week through observation under anesthesia with intraperitoneal injection of 0.15 mg/0.3 ml/20 g body weight pentobarbital (Dainihon Pharmaceutical Company, Osaka, Japan).

Rat anti-mouse Ifng neutralizing antibody was dissolved in PBS and injected subcutaneously into 10 alopecic lesions at a concentration of 0.4 mg/kg in 0.1 ml every day for a week. Rat IgG (DAKO Cytomation) was applied to the 10 alopecic lesions in the same protocol as a negative control. Hair growth was graded every week.

Hair Growth Grading

For each injected site, the percentage of hair surface coverage on alopecic skin was estimated. The quality and density of the hair were assessed and graded on a four-point scale (grade 0, no hair; grade 1, stubble, short broken hairs; grade 2, sparse intermediate length hairs; grade 3, normal length and density hairs) as described[14]. The percentage of hair coverage was multiplied by the quality/density grade for each area. Using this method, the hair growth index may thus range from 0 (no hair) to a maximum of 300 (100% normal hair).

Application of T-box21 Antisense Oligonucleotide

Antisense *Tbx21* oligonucleotide (5′-CTCCACGATGCCCATC-3′) and non-sense oligonucleotide (5′-CTATGTCATCCCGCTCCAC-3′) were purchased from Proligo (Kyoto, Japan). This antisense *Tbx21* oligonucleotide was reported to suppress *Tbx21* expression in the study by Lovett-Racke et al.[9] Antisense Tbx21 oligonucleotide and non-sense oligonucleotide were injected subcutaneously into six alopecic lesions, respectively, at a concentration of 0.5 mg/kg/day in 0.2 ml every 3 days for seven times. The hair growth index was calculated every week.

Preparation of Cationized Gelatin

The gelatin sample with an isoelectric point of 9.0 (molecular weight 100,000) prepared by an acid process of pig skin was kindly supplied by Nitta Gelatin Inc., Osaka, Japan. Ethylenediamine was obtained from Wako Pure Chemical, Ltd., Osaka, Japan. 2,4,6-Trinitrobenzene sulfonic acid, 1-ethyl-3-(3-dimethylaminopropyl) carbodiimide hydrochloride salt and 25 wt % glutaraldehyde aqueous solution were purchased from Nacalai Tesque, Kyoto Japan. The carboxyl groups of gelatin were chemically converted by introducing amino groups for cationization of gelatin.[8] Briefly, ethylenediamine and 1-ethyl-3-(3-dimethylaminopropyl) carbodiimide hydrochloride salt were added to 250 ml of 100 mmol/L PBS containing 5 g of gelatin. The molar ratio of ethylenediamine to the carboxyl groups of gelatin was 50. Immediately after this, the solution pH was adjusted to 5.0 by adding 5 mol/L HCl aqueous solution. The reaction mixture was agitated at 37°C for 18 hours and then dialyzed against double-distilled water for 48 hours at room temperature. The dialyzed solution was freeze-dried to obtain a cationized gelatin. The percentage of amino groups introduced into gelatin was 50.9 mol % per the carboxyl groups of gelatin.

Preparation of Cationized Gelatin Microspheres

Cationized gelatin microspheres were prepared by chemical cross-linking of gelatin in a water-in-oil emulsion state.[8] An aqueous solution of 10 wt % cationized gelatin (10 ml) was preheated at 40°C and then added dropwise into 375 ml of olive oil preheated at 40°C, while an impeller stirring at 420 rpm was used for 10 minutes to yield a water-in-oil emulsion. The emulsion temperature was decreased to 4°C followed by further stirring for 30 minutes for the natural gelation of gelatin aqueous solution. Ice-cold acetone (100 ml) was added to the emulsion and stirring was continued for 10 minutes. The resulting microspheres were washed three times with ice-cold acetone, collected by centrifugation (5000 rpm, 4°C, 5 minutes), fractionated in size by sieves with apertures of 70 and 100 μm, and air-dried at 4°C. The average diameter of microspheres used was 75 μm. The non-cross-linked and dried gelatin microspheres (50 mg) were placed in 25 ml of acetone/0.01 mol/L HCl solution (7:3, v/v) containing 60 μl of 25 wt % glutaraldehyde solution and stirred at 4°C for 24 hours to allow the cationized gelatin to cross-link. After washing by centrifugation (5000 rpm, 4°C, 5 minutes) with double-distilled water, the microspheres were agitated in 25 ml of 100 mmol/L aqueous glycine solution at room temperature for 1 hour to block the residual aldehyde groups of unreacted glutaraldehyde. The resulting microspheres were washed three times with double-distilled water by centrifugation and freeze-dried.

Application of Tbx21 siRNA

Tbx21 siRNA (5′-UGAUCGUCCUGCAGUCUCUdTdT-3′, 3′-dTdTACUAGCAGGACGUCAGAGA-5′) and non-sense

siRNA (5′-CGAACGAGUACCGUACACUdTdT-3′, 3′-dT-dTGCUUGCUCAUGGCAUGUGA-5′) were purchased from Proligo. This Tbx21siRNA suppressed Tbx21expression in the study by Lovett-Racke et al.[9] To impregnate Tbx21 siRNA into cationized gelatin microspheres, 10μl of PBS solution (pH 7.4) containing 10 μg of Tbx21 siRNA was dropped onto 1 mg of the freeze-dried cationized gelatin microspheres, kept overnight at 4°C, and injected subcutaneously into eight alopecic lesions in 0.2 ml of PBS every 7 days for three times. Ten micrograms of naked siRNA and 10 μg of cationized gelatin-conjugated nonsense siRNA were used as negative controls for eight alopecic lesions and eight alopecic lesions, respectively. The hair growth index was calculated every week.

Western Blotting

Skins from mice were washed three times in ice-cold PBS and homogenized in buffer containing 50 mmol/L Tris-HCl, pH 6.8, 20 mg/ml sodium dodecyl sulfate, 60 mg/ml β-mercaptoethanol, 100 mg/ml glycerol at a ratio of 300 μl lysis buffer to 100 mg of tissue. Total cell lysates were centrifuged at 13,000 rpm for 10 minutes. Supernatants were boiled for 5 minutes at 95°C and separated on 10% sodium dodecyl sulfate-polyacrylamide gel electrophoresis gels. Resolved protein was transferred to polyvinylidene difluoride membrane (Bio-Rad Inc., Hercules, CA) and blocked with 5% skim milk (Wako) at 4°C overnight. Blots were incubated with anti-mouse Tbx21 (4B10) antibody (1 μg/ml) (Santa Cruz Biotechnology, Santa Cruz, CA) or anti-Actb (AC-40) antibody (3 μg/ml) for 2 hours at room temperature. After three washes with PBS (10 minutes/wash), blots were incubated with horseradish peroxidase-conjugated goat anti-mouse Ig (P0447) (1:1000) (DAKO, Glostrup, Denmark) for 1 hour at room temperature. After three washes with PBS (10 minutes/wash), blots were incubated with ECL plus solution (GE Health Care, Buckinghamshire, UK) to visualize according to the manufacturer's instructions.

RNA Extraction and Real-Time PCR Assay

Total RNA from homogenized full-thickness back skin from C3H/HeJ mice was extracted using Qiagen RNeasy Mini Kit (Qiagen, Hilden, Germany) according to the protocol provided by the company and was reverse-transcribed into cDNA with a first strand cDNA synthesis kit RT-PCR (Roche Diagnostics, Indianapolis, IN). The expression levels of histocompatibility 2, class II antigen A, β1, actin β (*Actb*) were examined using 20X Assays-on-Demand Gene Expression Assay Mix (Mm00439216_m1, Mm00607939_s1, respectively, Applied Biosystems, Foster City, CA) with a 7300 system (Applied Biosystems) according to the manufacturer's instructions. The same difference was confirmed using glyceraldehyde-3-phosphate dehydrogenase gene (*GAPDH*) expression (Mm_99999915_g1) as a control (data not shown).

Results

CD4-Positive Lymphocytes Infiltrating around the Hair Follicles Are Dominantly CCR5-Positive

In patients with alopecia areata, ectopic major histocompatibility complex (MHC) class I and class II expression in the follicular epithelium leads to a collapse of immunoprivilege of hair follicles.[1] To elucidate the trigger of collapse of immunoprivilege, we examined the profile of infiltrating lymphocytes around the hair bulbs in peripheral region of alopecia areata at the active phase. Hairs surrounding the alopecic region could be plucked without any difficulty and revealed characteristic exclamation mark-like structures with tapering hair shafts in the most proximal region under a light microscope. Skin biopsies were taken from the peripheral region of alopecia areata, because those regions are considered to reveal strongest autoinflammatory reactions.[1]

Hematoxylin and eosin staining disclosed dense, so-called "swarm of bees"-like lymphocyte infiltrates around the hair bulbs (Figure 1A). To elucidate the character of the infiltrating CD4 T lymphocytes, serial frozen sections were stained with anti-CD4, anti-CCR5 (Th1 lymphocyte marker), and anti-CCR4 antibodies (Th2 lymphocyte marker) (Figure 1, B–E).[15] Immunohistochemistry revealed that infiltrative CD4-positive lymphocytes around the hair bulbs are mostly CCR5-positive cells with a few CCR4-positive cells (Figure 1, C–E). More than 80% of infiltrating CD4-positive cells are CCR5-positive, while 10% of CD4-positive cells are CCR4-positive (Figure 1F), suggesting that Th1 reaction is dominant in alopecia areata skin.

Il4 Applications Ameliorated Alopecia in Mouse Model C3H/HeJ Mice

Given the above result that Th1 reactions are dominant in human alopecia areata region, we investigated whether or not Th2 type cytokine recombinant Il4 injection could improve the alopecia in alopecia areata mouse model C3H/HeJ mice. C3H/HeJ mice refers to the rodent alopecia areata model.[16–19] C3H/HeJ mice develop hair loss spontaneously. The hair loss in C3H/HeJ mice and human alopecia areata have the common five characteristics: 1) alopecia occurs spontaneously; 2) both CD4-positive lymphocytes and CD8 lymphocytes infiltrate around the hair follicles; 3) ICAM-1 and MHC class I and MHC class II are ectopically expressed in the hair follicle epithelium; 4) autoreactive circulating antibodies against the hair follicles are existent; 5) topical immunotherapy with squaric acid dibutylester is effective for alopecia both in humans and C3H/HeJ mice.

Since intraperitoneal injections of 0.1 μg of recombinant Il4 suppressed delayed-type hypersensitivity reactions,[20] we used the same amount of Il4 in the present study. Intralesional injections of recombinant Il4 (0.1 μg) every day for 3 weeks significantly restored hair shaft elongations from alopecic skin of C3H/HeJ female mice when compared with the sodium chloride injections. (Fig-

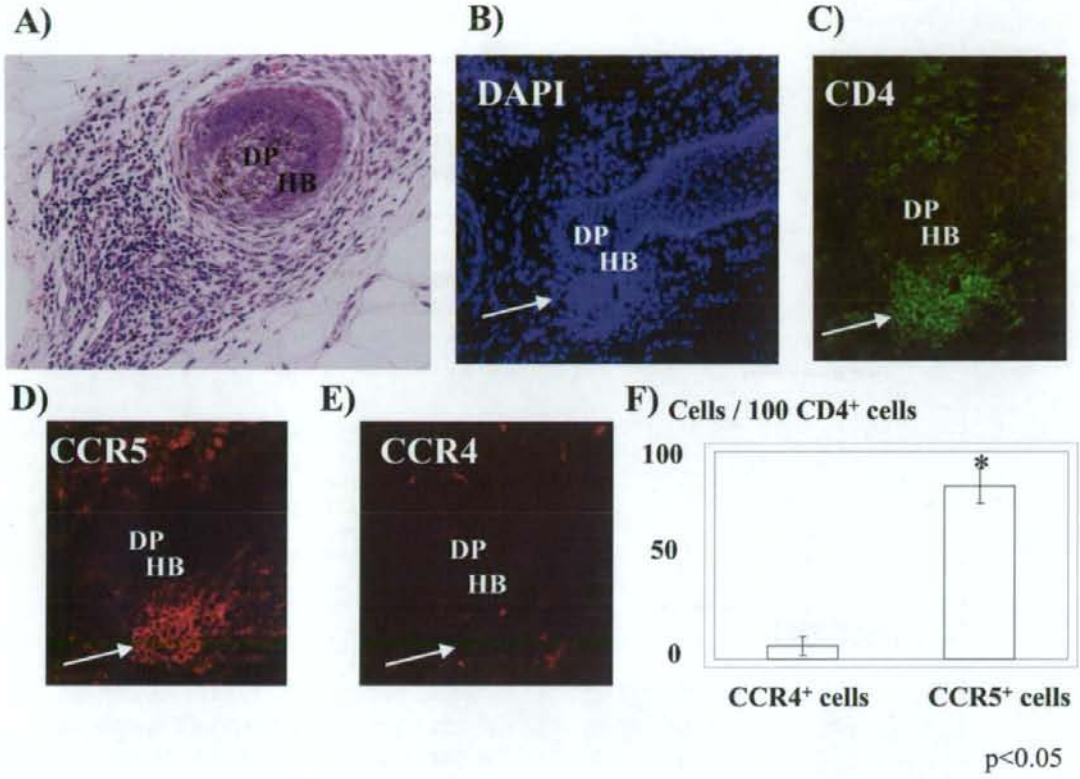

Figure 1. A: Hematoxylin and eosin staining of the section of alopecia areata patient. Dense lymphocytic infiltrates around the hair bulb. Immunohistochemical staining with 4',6-diamino-2-phenylindole (**B**), anti-CD4 (**C**), anti-CCR5 (**D**), and anti-CCR4 (**E**) antibody. Infiltrating lymphocytes were dominantly CCR5 positive (**arrows**). **F:** Percentage of CCR4-positive and CCR5-positive cells among CD4-positive cells. Predominance of CCR5-positive cells. DP, dermal papilla; HB, hair bulb. $^*P < 0.05$.

ure 2, A–C). There was no recurrence of alopecia from these mice during a 2-month observation period after the cessation of Il4 application. This Il4 effect was suppressed by the simultaneous injection of 0.01 μg of recombinant Ifng (Figure 2C).

To observe whether Il4 suppressed the CD8 T lymphocyte infiltration around the hair follicles, we performed immunohistochemistry with anti-CD8 antibody before and after injections. There were a lot of CD8-positive T lymphocyte infiltrates around the hair follicles as described (Figure 2D).[16] However, after Il4 applications, the number of CD8 T cell infiltrates around the hair follicles statistically significantly decreased (Figure 2, E and F).

Ifng Expression Level Is Elevated in the Alopecic Region in C3H/HeJ Mice and Suppressed by Intralesional Il4 Injections

To explore which cytokines are up-regulated or down-regulated in the alopecic region in C3H/HeJ mice, we performed semiquantitative RT-PCR using skin cDNA with Th1 cytokine, *Ifng* and IL-12b (*Il12b*), and Th2 cytokine *Il4* primers. In the alopecic skin, Th1 cytokine Ifng mRNA was expressed nine times stronger than in unaffected skin compared to β-actin (*Actb*) cytoplasmic expression as a control (Figure 3, A and D). Intralesional Il4 injections into the alopecic skin significantly suppressed the enhanced expression of Ifng mRNA (Figure 3, A and D). The expression level of Ifng mRNA in the Il4-injected skin returned to the same level as that in unaffected skin.

There was no statistically significant difference in the expression level of Il4 or Il12b mRNA between in alopecic skin and in unaffected skin (Figure 3, B and C). Furthermore, intralesional Il4 injections into the alopecic skin had no significant effect on the expression of Il4 or Il12b mRNA.

Intralesional Anti-Ifng Neutralizing Antibody Injections Were Effective Treatment for the Alopecia in Alopecia Areata Mouse Model C3H/HeJ Mice

The above result suggested that higher expression of Ifng mRNA expression in the alopecic skin might play an important rule in the pathogenesis of alopecia areata in

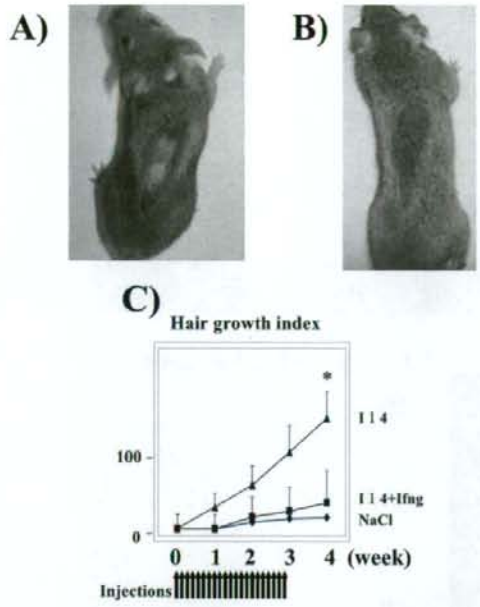

Figure 2. Alopecic skin lesion on the back of the C3H/HeJ mouse before (**A**) and after (**B**) recombinant Il4 injections. **C:** Hair growth index of alopecia with Il4, Il4 + Ifng and control NaCl injections (n = 10 each). CD8-positive cell infiltrates into the hair follicles before (**D**) and after (**E**) the Il4 injections. **F:** The number of CD8 T cell infiltrates per hair follicle was diminished after Il4 injections (n = 4 each). HS, hair shaft. $^*P < 0.05$.

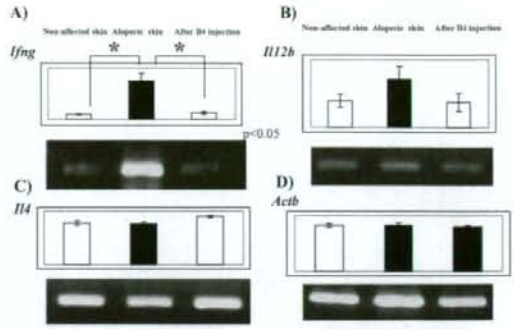

Figure 3. Expression of *Ifng* (**A**), *Il12b* (**B**), *Il4* (**C**), and *Actb* (**D**) mRNA in unaffected skin and alopecic skin. *Ifng* mRNA was suppressed by Il4 injections (**A**) (n = 3 each). $^*P < 0.05$.

C3H/HeJ mice. To determine whether blockade of Ifng actions in the skin leads to the restoration of the hair elongation, rat anti-neutralizing antibody against mouse Ifng was injected into the alopecic skin of the female C3H/HeJ mice. Anti-Ifng antibody injections improved the hair growth index more efficiently than the control rat IgG (Figure 4). There was no disappearance of hair shafts from these mice during a 2-month observation period after the cessation of antibody application.

Intralesional Injections of Tbx21 Antisense Oligonucleotide Were Effective Treatment for the Alopecia in Alopecia Areata Mouse Model C3H/HeJ Mice

Tbx21 (formerly known as T-bet) is a T-box containing transcription factor and indispensable for Th1 differentiation. This protein binds to the promoter of *Ifng* gene and augments its expression. To examine a role of *Tbx21* in the pathogenesis of alopecia areata, we subcutaneously injected antisense *Tbx21* oligonucleotide into female C3H/HeJ mice alopecic lesions every other day for seven times. Although the effect of antisense *Tbx21* oligonucleotide took place more slowly than Il4 or neutralizing anti-Ifng antibody (Figures 2, 4, and 5), antisense *Tbx21* oligonucleotide was significantly more effective for alopecia than non-sense oligonucleotide (Figure 5). There was no disappearance of hair shafts from these mice

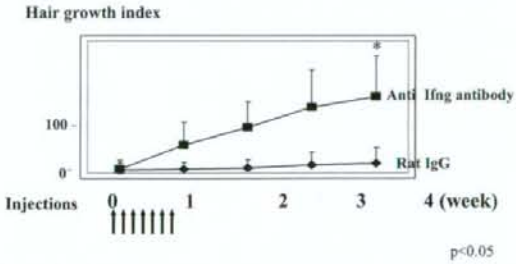

Figure 4. Hair growth index of alopecia with rat neutralizing anti-Ifng antibody and control rat IgG injections (n = 8 each). $^*P < 0.05$.

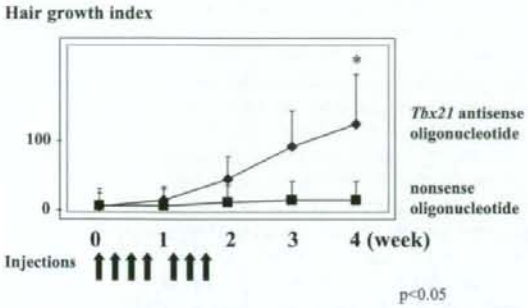

Figure 5. Hair growth index of alopecia with *Tbx21* antisense oligonucleotide and non-sense oligonucleotide injections ($n = 6$ each). $^*P < 0.05$.

during a 2-month observation period after the cessation of antisense oligonucleotide application.

Intralesional Injections of Tbx21 siRNA Conjugated with Cationized Gelatin Were Effective Treatment for the Alopecia in Alopecia Areata Mouse Model C3H/HeJ Mice

To decrease the number of injections, we introduced a new drug delivery system, that is, a controlled release of siRNA conjugated with a biodegradable cationized gelatin. After conjugation of siRNA with the cationized gelatin at 4°C overnight, we subcutaneously injected siRNA conjugated with cationized gelatin once a week three times. Cationized gelatin is gradually processed in the skin, and, in turn, released siRNA binds sequence-specifically to mRNA. Cationized gelatin-conjugated *Tbx21* siRNA injections were more effective than naked *Tbx21* siRNA injections or non-sense siRNA conjugated with cationized gelatin (Figure 6B). There was no recurrence of alopecia in the mice during a 2-month observation period after the cessation of *Tbx21* siRNA application. The result suggests that controlled release of siRNA with a biodegradable cationized gelatin effectively worked *in vivo*.

Controlled Release of Tbx21 siRNA Suppressed Tbx21 Protein Expression in Skin

To investigate whether controlled release of *Tbx21* siRNA in skin really suppressed the Tbx21 protein expression, we checked the Tbx21 expression level by Western blotting. Tbx21 protein expression was indeed suppressed by the controlled release of *Tbx21* siRNA (Figure 6A). The similar intensity of the control Actb band between before and after *Tbx21*siRNA injections indicated that suppression of mRNA expression by *Tbx21* siRNA was gene-specific.

Controlled Release of Tbx21 siRNA Suppressed MHC Class II Expression in Alopecic Skin

Since ectopic expression of MHC class I and MHC class II in the hair follicles may destroy the immune privilege of

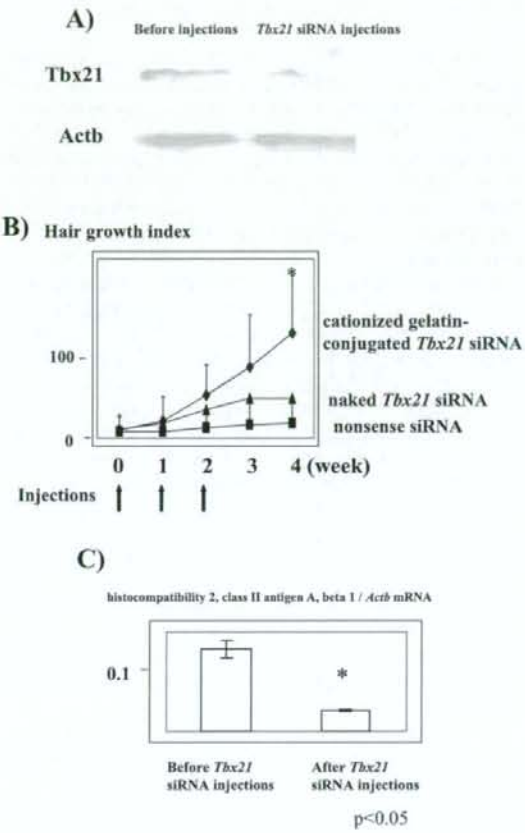

Figure 6. A: Western blotting of skin lysates before and after cationized gelatin-conjugated *Tbx21* siRNA injections. Tbx21 protein expression was suppressed after cationized gelatin-conjugated *Tbx21* siRNA injections, while control Actb protein expression remained at the same level. **B:** Hair growth index of alopecia with cationized gelatin-conjugated *Tbx21* siRNA, naked *Tbx21* siRNA, and control cationized gelatin-conjugated non-sense siRNA injections ($n = 8$ each). $^*P < 0.05$. **C:** Histocompatibility 2, class II antigen A, $\beta 1$ mRNA expression in alopecic skin measured with real-time PCR was suppressed by cationized gelatin-conjugated *Tbx21* siRNA injections ($n = 4$ each). $^*P < 0.05$.

hair follicles, we explored the expression change of histocompatibility 2, class II antigen A, $\beta 1$ mRNA after the *Tbx21* siRNA injections. Real-time RT-PCR study revealed that controlled release of *Tbx21* siRNA suppressed histocompatibility 2, class II antigen A, $\beta 1$ mRNA expression in alopecic skin (Figure 6C). This result suggests a restoration of immune privilege of hair follicles after *Tbx21* siRNA injections.

Discussion

Alopecia areata is an autoimmune disease that sometimes evolves into alopecia totalis affecting the whole scalp.[1] This severe type of alopecia tends to be resistant to conventional therapies such as topical immunotherapy with squaric acid dibutylester or diphenylcyclopropenone, oral steroid intake, psoralen plus ultraviolet A treat-

ment, or topical steroid application. Therefore, these patients wait for a new therapy.

Cytokine therapy is a novel therapeutic approach for alopecia areata resistant to previous therapies, since cytokine therapy has already been proved to be effective for a skin inflammatory disease, psoriasis vulgaris.[21,22] Psoriasis vulgaris is a hyperproliferative skin disease in which Th1 lymphocytes predominantly infiltrate in the dermis. Systemic Il4 injections are effective for amelioration of psoriasis vulgaris.[21] In our study, we demonstrated that infiltrating CD4 lymphocytes around the hair follicles are mostly CCR5-positive cells indicating that these cells are Th1 CD4 lymphocytes (Figure 1). The injection of Th2 cytokine, Il4, intralesionally instead of systematically, resulted in hair shaft elongation through the suppression of CD8 T lymphocyte infiltrates around the hair follicles (Figure 2). Alopecia areata is usually limited to the head and, hence, it serves a good candidate for a local injection. Local administration of cytokines might be better than a systemic administration of cytokines for the following reasons: 1) a required dose might be smaller; 2) systemic side effects might be less; and 3) topical application is easier than systemic administration. Biedermann et al demonstrated that more than three intraperitoneal Il4 injections per day was necessary to improve delayed-type hypersensitivity reactions[20] in contrast to a single subcutaneous injection per day in our study. Drug delivery of Il4 and half-time of Il4 decay may be different due to the means of application.

In our study, intralesional injections of Il4 suppressed an enhanced expression of *Ifng* in alopecic skin (Figure 3). In a previous study, when Ifng was injected into non-alopecic genetically susceptible C3H/HeJ mice, alopecia was induced with an ectopic expression of MHC class I and class II on follicular epithelium.[19] Our study demonstrated that anti-Ifng neutralizing antibody injections ameliorated alopecia in C3H/HeJ mice (Figure 4). Taken together, Ifng plays a pivotal role both in the induction and the maintenance of alopecia in genetically susceptible C3H/HeJ mice.

Gene therapy is a new therapeutic approach for intractable alopecia areata. To establish a gene therapy for a rodent alopecia areata model C3H/HeJ mice, we focused on *Tbx21* gene. Tbx21 plays a key role in Th1 cell development.[9] Tbx21 deficient mice revealed a defect in Th1 immune reaction.[9] Moreover, a recent study showed that Tbx21 binds to a distal conserved sequence element of *Ifng* gene and enhances *Ifng* gene expression.[10] Our study demonstrated that intralesional injections of *Tbx21* antisense oligonucleotide restored the hair shaft elongation in alopecia areata model C3H/HeJ mice (Figure 5). Therefore, local injection of *Tbx21* antisense oligonucleotide may exert similar effects on alopecia by suppressing the expression of *Ifng*.

RNA interference by siRNA is a recently developed powerful technique to suppress the expression of certain genes with a high specificity.[5] The gene delivery system is generally divided into two categories: viral and nonviral vectors. Although viral vectors such as retrovirus, adenovirus, and adeno-associated virus are potentially efficient, nonviral vectors have the advantages of less toxicity, less immunogenicity, and easier preparation.[8] So far, several methods for delivering genes with nonviral carriers have been developed, including naked plasmid DNA injection and complex formation with cationized polymers or cationized liposomes. However, there are several drawbacks with each nonviral vector, including a low efficiency of gene transfection compared with viral vectors and a transient gene expression. In this study, we introduce a system of prolonged release of siRNA from cationized gelatin microspheres. The controlled release of the siRNA may prevent rapid degradation of DNA and facilitate exposure and transduction of siRNA to cells. Moreover, the *in vivo* enzymatic degradation of gelatin microspheres depends on their cross-linking extent, which can be regulated by changing the concentration of glutaraldehyde used for microsphere preparation.

Cationized gelatin used in our study is a very safe molecule for human beings. Comparison between the cationized gelatin-conjugated siRNA and naked siRNA in our study revealed that controlled delivery of siRNA with cationized gelatin was indeed more efficient for alopecia than naked siRNA (Figure 6B). It is likely that naked siRNA is more easily degraded by nuclease than siRNA conjugated with cationized gelatin.

Trial of the treatment with controlled delivery of siRNA for skin diseases has several advantages over usage of siRNA for other organ diseases. First, local applications of siRNA to skin lesions are very easy. Second, the cutaneous changes induced by siRNA application can be observed without any difficulty or expensive machines. Third, pathological changes can be assessed easily by skin biopsies.

The drug delivery system is totally different between human skin and mouse skin. Moreover, the mouse model used in our study shows a number of differences to human alopecia areata. Before application of this siRNA delivery system into therapeutic use for human alopecia areata, these points should be carefully and critically assessed.

In conclusion, we have developed an efficient and safe method for *Tbx21* siRNA delivery to alopecic skin and demonstrated specific inhibition of target gene expression resulting in a restoration of hair shaft elongation. To our knowledge, this is the first report of effective controlled delivery of siRNA using biodegradable cationized gelatin in animal models of diseases.

References

1. Paus R, Nickoloff BJ, Ito T: A "hairy" privilege. Trends Immunol 2005, 26:32–40
2. Ito T, Ito N, Bettermann A, Tokura Y, Takigawa M, Paus R: Collapse and restoration of MHC class-I-dependent immune privilege: exploiting the human hair follicle as a model. Am J Pathol 2004, 164:623–634
3. Gilhar A, Ullman Y, Berkutzki T, Assy B, Kalish RS: Autoimmune hair loss (alopecia areata) transferred by T lymphocytes to human scalp explants on SCID mice. J Clin Invest 1998, 101:62–67
4. Gilhar A, Landau M, Assy B, Shalaginov R, Serafimovich S, Kalish RS: Mediation of alopecia areata by cooperation between $CD4^+$ and $CD8^+$ T lymphocytes. Arch Dermatol 2002, 138:916–922

5. Hannon GJ, Rossi JJ: Unlocking the potential of the human genome with RNA interference. Nature 2004, 431:371–378
6. Takeshita F, Minakuchi Y, Nagahara S, Honma K, Sasaki H, Hirai K, Teratani T, Namatame N, Yamamoto Y, Hanai K, Kato T, Sano A, Ochiya T: Efficient delivery of small interfering RNA to bone-metastatic tumors by using atelocollagen in vivo. Proc Natl Acad Sci 2005, 102:12177–12182
7. Palliser D, Chowdhury D, Wang QY, Lee SJ, Bronson RT, Knipe DM, Lieberman J: An siRNA-based microbicide protects mice from lethal herpes simplex virus 2 infection. Nature 2006, 439:89–94
8. Kushibiki T, Matsumoto K, Nakamura T, Tabata Y: Suppression of tumor metastasis by NK4 plasmid DNA released from cationized gelatin. Gene Ther 2004, 11:1205–1214
9. Lovett-Racke AE, Rocchini AE, Choy J, Northrop SC, Hussain RZ, Ratts RB, Sikder D, Racke MK: Silencing T-bet defines a critical role in the differentiation of autoreactive T lymphocytes. Immunity 2004, 21:719–731
10. Hatton RD, Harrington LE, Luther RJ, Wakefield T, Janowski KM, Oliver JR, Lallone RL, Murphy KM, Weaver CT: A distal conserved sequence element controls *Ifng* gene expression by T cells and NK cells. Immunity 2006, 25:717–729
11. Olsen E, Hordinsky M, McDonald-Hull S, Price V, Roberts J, Shapiro J, Stenn K: Alopecia areata investigational assessment guidelines. J Am Acad Dermatol 1999, 40:242–246
12. Nakamura M, Matzuk MM, Gerstmayer B, Bosio A, Lauster R, Miyachi Y, Werner S, Paus R: Control of pelage hair follicle development and cycling by complex interactions between follistatin and activin. FASEB J 2003, 17:497–499
13. Hayashi M, Higashi K, Kato H, Kaneko H: Assessment of preferential Th1 or Th2 induction by low-molecular-weight compounds using a reverse transcription-polymerase chain reaction method: comparison of two mouse strains C57BL/6 and Balb/c Toxicol Appl Pharmacol 2001, 177:38–45
14. Tang L, Cao L, Sundberg JP, Lui H, Shapiro J: Restoration of hair growth in mice with an alopecia areata-like disease using topical anthralin. Exp Dermatol 2004, 13:5–10
15. Uchida T, Suto H, Ra C, Ogawa H, Kobata T, Okumura K: Preferential expression of Th2-type chemokine and its receptor in atopic dermatitis. Int Immunol 2002, 14:1431–1438
16. Sundberg JP, Cordy WR, King LE: Alopecia areata in aging C3H/HeJ mice. J Invest Dermatol 1994, 102:847–856
17. Freyschimidt-Pual P, Sundberg JP, Happle R, McElwee KJ, Metz S, Boggess D, Hoffmann R: Successful treatment of alopecia areata-like hair loss with the contact sensitizer squaric acid dibutylester (SADBE) in C3H/HeJ mice. J Invest Dermatol 1999, 113:61–68
18. McElwee KJ, Hoffmann R, Freyschimidt-Pual P, Wenzel E, Kissling S, Sundberg JP, Zöller M: Resistance to alopecia areata in C3H/HeJ mice is associated with increased expression of regulatory cytokines and a failure to recruit $CD4^+$ and $CD8^+$ cells. J Invest Dermatol 2002, 119:1426–1433
19. Gilhar A, Kam Y, Assy B, Kalish RS: Alopecia areata induced in C3H/HeJ mice by interferon-γ: evidence for loss of immune privilege. J Invest Dermatol 2005, 124:288–289
20. Biedermann T, Mailhammer R, Mai A, Sander C, Ogilvie A, Brombacher F, Maier K, Levine AD, Röcken M: Reversal of established delayed type hypersensitivity reactions following therapy with IL-4 or antigen-specific Th2 cells. Eur J Immunol 2001, 31:1582–1591
21. Ghoreschi K, Thomas P, Breit S, Dugas M, Mailhammer R, van Eden W, van der Zee R, Biedermann T, Prinz J, Mack M, Mrowietz U, Christophers E, Schlöndorff D, Plewig G, Sander CA, Röcken M: Interleukin-4 therapy of psoriasis induces Th2 responses and improves human autoimmune disease. Nat Med 2003, 9:40–46
22. Racke MK, Bonomo A, Scott DE, Cannella B, Levine A, Raine CS, Shevach EM, Röcken M: Cytokine-induced immune deviation as a therapy for inflammatory autoimmune disease. J Exp Med 1994, 180:1961–1966

Plectin 1 links intermediate filaments to costameric sarcolemma through β-synemin, α-dystrobrevin and actin

Takao Hijikata[1,*], Akio Nakamura[2], Keitaro Isokawa[3], Michihiro Imamura[4], Katsutoshi Yuasa[1], Ryoki Ishikawa[2], Kazuhiro Kohama[2], Shinichi Takeda[4] and Hiroshi Yorifuji[5]

[1]Department of Anatomy and Cell Biology, Faculty of Pharmacy, Research Institute of Pharmaceutical Sciences, Musashino University, Tokyo 202-8585, Japan
[2]Department of Molecular and Cellular Pharmacology, Gunma University Graduate School of Medicine, Gunma 371-8511, Japan
[3]Department of Anatomy, Nihon University School of Dentistry, Tokyo 101-8310, Japan
[4]Department of Molecular Therapy, National Institute of Neuroscience, NCNP, Tokyo 187-8502, Japan
[5]Department of Anatomy, Gunma University Graduate School of Medicine, Gunma 371-8511, Japan
*Author for correspondence (e-mail: hijikata@musashino-u.ac.jp)

Accepted 19 March 2008
Journal of Cell Science 121, 2062-2074 Published by The Company of Biologists 2008
doi:10.1242/jcs.021634

Summary

In skeletal muscles, the sarcolemma is possibly stabilized and protected against contraction-imposed stress by intermediate filaments (IFs) tethered to costameric sarcolemma. Although there is emerging evidence that plectin links IFs to costameres through dystrophin-glycoprotein complexes (DGC), the molecular organization from plectin to costameres still remains unclear. Here, we show that plectin 1, a plectin isoform expressed in skeletal muscle, can interact with β-synemin, actin and a DGC component, α-dystrobrevin, in vitro. Ultrastructurally, β-synemin molecules appear to be incorporated into costameric dense plaques, where they seem to serve as actin-associated proteins rather than IF proteins. In fact, they can bind actin and α-dystrobrevin in vitro. Moreover, in vivo immunoprecipitation analyses demonstrated that β-synemin- and plectin-immune complexes from lysates of muscle light microsomes contained α-dystrobrevin, dystrophin, nonmuscle actin, metavinculin, plectin and β-synemin. These findings suggest a model in which plectin 1 interacts with DGC and integrin complexes directly, or indirectly through nonmuscle actin and β-synemin within costameres. The DGC and integrin complexes would cooperate to stabilize and fortify the sarcolemma by linking the basement membrane to IFs through plectin 1, β-synemin and actin. Besides, the two complexes, together with plectin and IFs, might have their own functions as platforms for distinct signal transduction.

Supplementary material available online at
http://jcs.biologists.org/cgi/content/full/121/12/2062/DC1

Key words: Costamere, Dystrobrevin, Dystrophin-glycoprotein complex, Plectin, Synemin

Introduction

Skeletal muscle fibers possess heteropolymeric intermediate filaments (IFs) comprised of desmin, synemin, and paranemin (Bilak et al., 1998; Granger and Lazarides, 1980; Price and Lazarides, 1983; Schweitzer et al., 2001). These IFs are located at the periphery of myofibrillar Z-discs, interlink adjacent myofibrils at the Z-line level, and anchor onto costameres beneath the sarcolemma (Craig and Pardo, 1983; Fujimaki et al., 1986; Lazarides, 1980; Tokuyasu et al., 1983). The importance of IF-interlinkages between adjacent Z-discs and IF-anchorage on costameric sarcolemma in muscle function and integrity is supported by investigations of desmin-knockout mice, in which muscle fibers lacking desmin IFs develop reduced maximum force and their sarcolemmae are more susceptible to damage during contraction (Balogh et al., 2003; Li et al., 1996; Li et al., 1997; Sam et al., 2000). However, molecular organization of the linkages from IFs to Z-discs and costameres still remains unclear.

Within costameres, dystrophin-glycoprotein complex (DGC) provides structural support to the sarcolemma by linking the actin-based cytoskeleton with the extracellular matrix (ECM) (for a review, see Ozawa, 2006). It is comprised of dystrophin, α- and β-dystroglycan, sarcoglycans, sarcospan, α-dystrobrevin and syntrophin. Dystrophin is associated with β-dystroglycan and extracellular α-dystroglycan, which in turn binds laminin-2 in the basement membrane (BM) (Ervasti and Campbell, 1993), while it is indirectly associated with a group of five integral membranous proteins, the sarcoglycans and sarcospan (Ozawa et al., 1998; Yoshida et al., 1994). Other subsarcolemmal proteins in the complex include α-dystrobrevin and syntrophin, which directly interact with dystrophin (Ahn et al., 1996; Sadoulet-Puccio et al., 1997).

β-Synemin is a constituent of heteropolymeric IF in muscles, and has a very short N-terminal head domain, a central α-helical rod domain conserved in all IF proteins, and a very long C-terminal tail domain (Titeux et al., 2001). β-synemin molecules are assumed to link IFs to DGC, based on the in vitro findings that they can bind α-dystrobrevin, dystrophin and desmin (Bhosle et al., 2006; Mizuno et al., 2001). However, their binding sites for desmin, α-dystrobrevin and dystrophin are all confined to their rod domains, thereby raising a possibility that heteropolymerization of β-synemin with desmin may prevent β-synemin from binding α-dystrobrevin and/or dystrophin and therefore from linking IFs to DGC due to their competition for the rod domains.

Another candidate for the linker between IFs and costameres is the versatile crosslinker protein plectin. Plectin harbors a binding site for IF proteins at its C-terminus (Foisner et al., 1988; Nikolic et al., 1996; Reipert et al., 1999), whereas its N-terminal parts include binding domains for actin and integrin β4 (Andra et al., 1998; Geerts et al., 1999; Rezniczek et al., 1998). With these binding properties, plectin links cytokeratin IFs to the plasma membrane at hemidesmosomes of epidermal cells (Hieda et al., 1992; Litjens et al., 2006). By analogy, it is conceivable that plectin links desmin IFs to costameric sarcolemma. In fact, our previous immunoelectron microscopic study ultrastructurally revealed that plectin-labeled fine threads linked IFs to dystrophin- or vinculin-containing subsarcolemmal dense plaques, or costameres (Hijikata at al., 2003). In that study, however, we did not identify plectin-binding partners within costameres and, therefore, could not fully explore molecular organization from IFs to costameres through plectin.

To address these unexplored subjects, the present study was undertaken just to identify β-synemin as a protein binding plectin N-terminal fragments. The present immuno-EM analyses revealed that β-synemin was incorporated into costameric dense plaques associated with plectin threads. Furthermore, our in vitro analyses showed that β-synemin could bind actin as well as α-dystrobrevin, whereas plectin 1 – a plectin isoform expressed in skeletal muscles – could interact with α-dystrobrevin, β-synemin and actin. Based on the results obtained here, we propose a model of molecular organization from IF to costameres that includes DGC and integrin complexes.

Results

Identification of β-synemin as a plectin-1-binding protein

Our previous immunoelectron microscopic analysis of rat skeletal muscle fibers revealed that plectin-labeled fine threads extended from desmin IFs to subsarcolemmal dense plaques containing dystrophin (Hijikata et al., 2003). Given this and the desmin-binding property of plectin at its C-terminus (Reipert et al., 1999), N-terminal parts of plectin would be expected to interact with as yet unidentified molecules within dystrophin-containing dense plaques. Thus, N-terminal fragments of plectin 1, an isoform of plectin expressed in skeletal muscles (Fuchs et al., 1999), were used as a probe for blot overlay assay to identify plectin-1-binding proteins within the subsarcolemmal dense plaques. The crude IF fraction prepared from muscle light microsome (LM) with detergents was separated by SDS-PAGE and blotted onto PVDF membranes. The membranes were overlaid with Myc-tagged N-terminal plectin-1-recombinant proteins (PleN1, 1-1273 aa), followed by detection of plectin-binding proteins with anti-Myc antibody. This blot overlay assay detected some Myc-positive bands representing possible plectin-1-binding proteins (data not shown).

Of these possible plectin-1-binding proteins, we focused our analysis on a protein of ~160 kDa (supplementary material Fig. S1A). We determined its partial amino acid sequence and found that it contained PHEFH and VQLQRMVDQRS sequences. These amino acid sequences were used to search the GenBank database using BLASTP for similar sequences. The two sequences were identical to those of KIAA0353, an incomplete cDNA sequence isolated from a human brain cDNA library (GenBank™ accession number AB002351). To obtain the full-length cDNA, cloning of the 160 kDa plectin-1-binding protein was performed in a cDNA library prepared from skeletal muscle mRNA of newborn rats. By determining the complete DNA sequences of the obtained clones, we identified the plectin-1-binding protein as desmuslin (GenBank accession number AB091769). Desmuslin, a novel member of IF proteins, was found as a α-dystrobrevin-binding protein by the yeast-two-hybrid system (Mizuno et al., 2001). Comparison of the previously reported human and the present rat sequences revealed an overall identity of 72.4%. Desmuslin has subsequently been referred to as β-synemin (Mizuno et al., 2004; Titeux et al., 2001), and this name is also used in this article. The interactions of plectin with β-synemin and then α-dystrobrevin, a dystrophin-associated protein, agreed with our previous findings of the association of plectin threads with dystrophin-containing dense plaques.

Plectin 1 interacts with β-synemin in vitro and in vivo

In vitro interactions between plectin and β-synemin were further verified by pull-down assays using recombinant plectin 1 and β-synemin proteins. GST-fused full-length β-synemin was incubated with either Myc-tagged N-terminal plectin 1 (PleN1) fragments or Myc-tagged β-galactosidase (LacZ) and then immunoprecipitated by using anti-Myc antibody and protein L-agarose. The results indicated that PleN1 fragments coimmunoprecipitated with β-synemin, but neither LacZ nor PleN1 did this in combination with control IgG (supplementary material Fig. S1B). A reciprocal pull-down assay was performed using glutathione beads. GST-fused β-synemin pulled down PleN1, but not LacZ, whereas GST protein alone did not precipitate PleN1 (supplementary material Fig. S1C).

For in vivo analysis, plectin or β-synemin immune complex was immunoprecipitated from lysates of muscle LM using anti-plectin or anti-β-synemin antibody, respectively. Subsequent immunoblotting for β-synemin or plectin indicated that plectin and β-synemin formed protein complexes in vivo as well (supplementary material Fig. S1D). In control experiments, neither plectin nor β-synemin was immunoprecipitated by control IgG.

Localization of β-synemin with plectin and α-dystrobrevin at costameric sarcolemma

To assess the localization of β-synemin relative to plectin and α-dystrobrevin in skeletal muscle, rat diaphragm cryosections were doubly immunolabeled with anti-β-synemin and anti-plectin or anti-α-dystrobrevin antibodies, and observed by confocal laser scanning microscopy. As shown in Fig. 1A-C, β-synemin completely colocalized with plectin, which was found around Z-discs and beneath the sarcolemma (Hijikata et al., 1999; Hijikata et al., 2003; Schröder et al., 1997; Schröder et al., 1999). On longitudinal sections, both β-synemin and plectin displayed striated staining of Z-lines and subsarcolemmal intermittent staining confined to areas overlying Z-lines or costameres (Fig. 1D-F). By contrast, α-dystrobrevin was more diffusely distributed along the sarcolemma (Fig. 1H,K,N,Q). Doubly immunostained tangential sections including the sarcolemma clearly delineated costameric striations coinciding between β-synemin and α-dystrobrevin (Fig. 1J-L), whereas the longitudinal sections displayed intermittent superimposition of β-synemin-staining on diffuse α-dystrobrevin-staining along the sarcolemma (Fig. 1M-O). Consistent with the present observation of its complete colocalization with β-synemin, plectin also colocalized with α-dystrobrevin at costameres (Fig. 1P-R). These results indicated the colocalization of β-synemin and plectin with α-dystrobrevin at the costameric sarcolemma.

To further explore the precise localization of β-synemin beneath the sarcolemma, immunogold electron microscopy (EM) analysis was performed in rat skeletal muscle fibers chemically skinned with saponin. In this EM analysis, specific gold particles indicative of

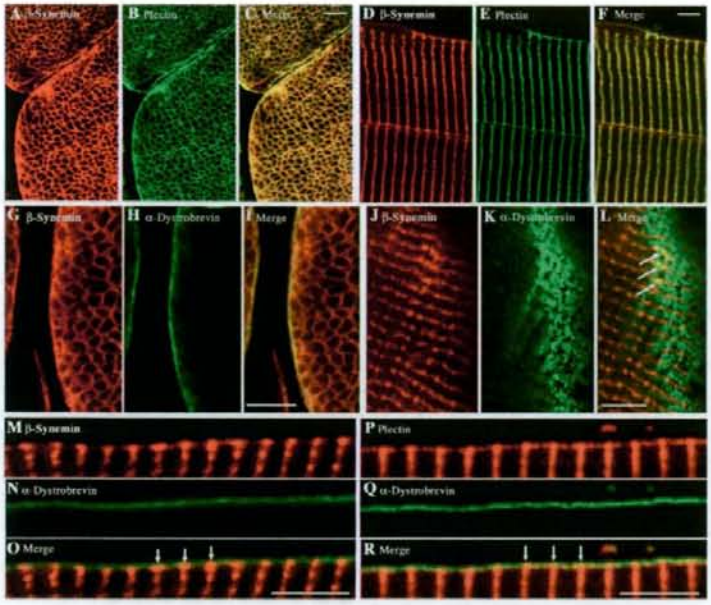

Fig. 1. (A-R) Colocalization of β-synemin with plectin and α-dystrobrevin at the costameric sarcolemma. β-Synemin colocalized precisely with plectin around Z-discs and beneath the sarcolemma (A-F), whereas it colocalized with α-dystrobrevin beneath the sarcolemma (G-O), especially at costameric regions (L,O, arrows). Plectin also colocalized with α-dystrobrevin at costameres (P-R, arrows in R). Bars, 5 μm.

β-synemin were found along IFs, on the cytoplasmic side of subsarcolemmal dense plaques overlying Z-lines, namely costameres, and between IFs and costameric dense plaques (Fig. 2). The association of β-synemin-specific gold particles along IFs was consistent with the notion that β-synemin, together with desmin and paranemin, formed heteropolymeric IF (Hemken et al., 1997; Hirako et al., 2003). Extensive observations disclosed that IFs were interlinked with costameric dense plaques by fine threads, possibly plectin molecules, on both sides of which β-synemin labels were localized (Fig. 2C). Costameric dense plaques without association of IF were also immunolabeled with the gold particles (Fig. 2B). These results indicated discrete incorporation of β-synemin molecules into two distinct sites: IFs and costameric dense plaques.

Mapping of subdomains interacting between plectin 1 and β-synemin

Pull-down assay was carried out to define more precisely the β-synemin subdomains involved in the interaction with PleN1. Based on the β-synemin domain structure consisting of head, rod and tail domains, ten β-synemin mutant recombinant proteins were generated by subcloning rat β-synemin cDNA into a GST expression system (Fig. 3A). These mutant β-synemin proteins were incubated with Myc-tagged PleN1 and pulled down using anti-Myc antibody and protein L-agarose. The mutant proteins (Tail N1, N2 and Rod C), including the N-terminal part of β-synemin tail domains, were pulled down using PleN1. In addition, mutant proteins (Rod Ms and Ml) including the C-terminal part of the rod domain (rod domain 2B) were also precipitated, but in smaller amounts. Without anti-Myc antibody, however, none of the β-synemin mutant proteins were pulled down. These results indicated that the part of β-synemin around the boundary between its rod and tail domains preferentially interacted with PleN1.

Next, to refine β-synemin-interacting sites on PleN1, reciprocal pull-down experiments were performed using GST-fused N-terminal tail fragments of β-synemin (Tail N1) and a variety of mutant plectin recombinant fragments, as shown in Fig. 3B. β-Synemin Tail N1 fragments precipitated mutant plectin 1 fragments, including the

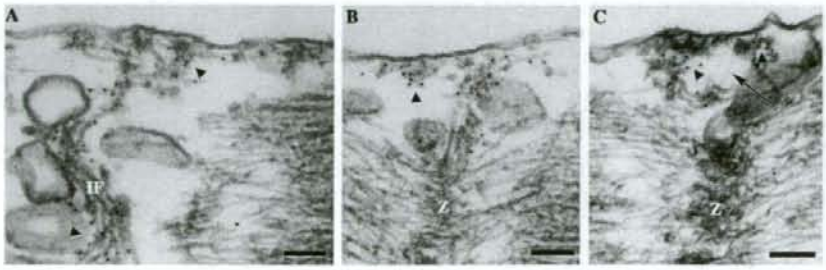

Fig. 2. Immunoelectron microscopic analyses indicate the localization of β-synemin along IFs and in costameres. (A,B) Gold particles labeling β-synemin (arrowheads) were distributed along IFs and on subsarcolemmal dense plaques overlying Z-lines, or costameres. (C) A thin thread (arrow), possibly plectin molecules, projects from IF to a dense plaque labeled with gold particles. Bars, 0.1 μm.

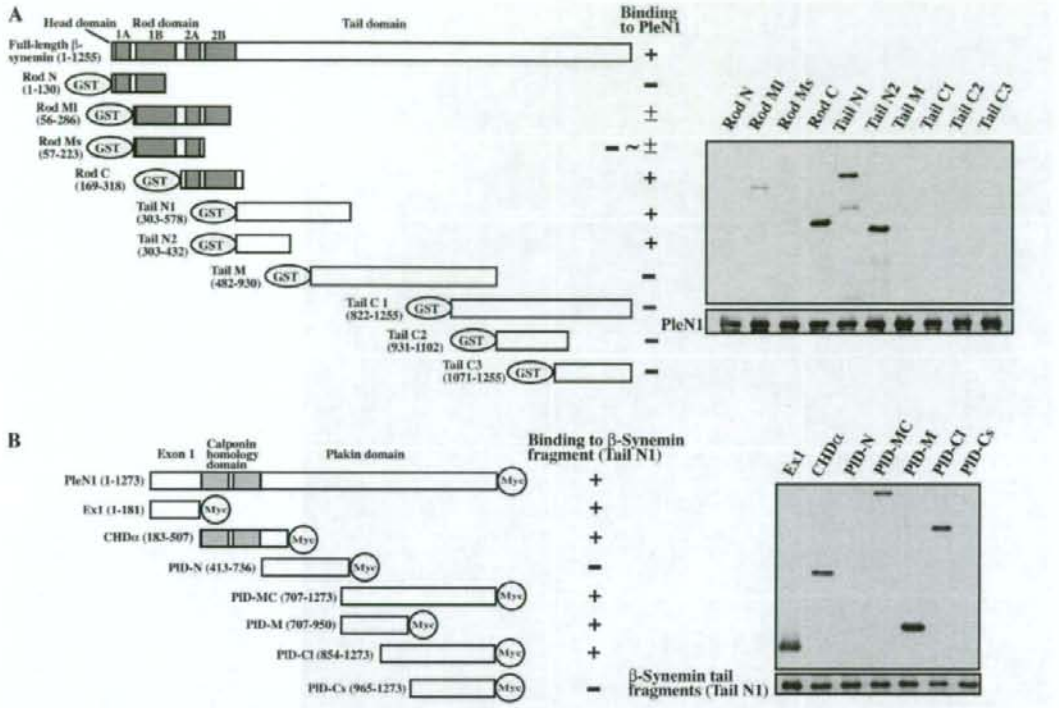

Fig. 3. Mapping of the interacting sites between N-terminal plectin 1 (PleN1) fragments and full-length β-synemin by in vitro pull-down assay. (A) Schematic representations of the domain structures of full-length β-synemin and GST-fused recombinant β-synemin fragments used in the pull-down assay. The in vitro PleN1-binding phenotypes of mutant β-synemin fragments are summarized as + (strong binding) or ± (weak binding). GST-fused β-synemin fragments were incubated with Myc-tagged PleN1 and immunoprecipitated by anti-Myc antibody and protein L-agarose. These immunoprecipitates were subjected to immunoblotting with detection by anti-GST antibody. Each lane contained equivalent amounts of the immunoprecipitate, as represented by immunoblots of PleN1. (B) Domain structures of PleN1 and Myc-tagged recombinant plectin fragments, together with a summary of in vitro binding ability of plectin fragments to β-synemin tail fragments (Tail N1). Plectin fragments were incubated with GST-fused Tail N1 and pulled down using glutathione beads, followed by immunoblotting with anti-Myc antibody. Each lane contained equivalent amounts of the immunoprecipitate, as represented by immunoblots of Tail N1.

first exon product, calponin-homology domains and the middle portion of plakin domain (Fig. 3B), indicating that PleN1 fragments included three β-synemin-binding sites.

Subcellular localization of mutant plectin fragments relative to β-synemin in C2C12 cells

The present mapping revealed that three mutant plectin 1 fragments, Ex1, CHDα and PlD-M could interact with β-synemin in vitro. To further assess these interactions within cells, we expressed the three Myc-tagged plectin fragments in C2C12 myoblasts and myotubes, and examined their subcellular localization relative to β-synemin by double immunostaining with anti-Myc and anti-β-synemin antibodies. Before the transfection experiments, we examined subcellular localization of β-synemin by immunohistochemistry using anti-β-synemin antibody and fluorescent phallotoxins in C2C12 myoblasts and myotubes. In most of C2C12 myoblasts, β-synemin was expressed in a diffuse dotted pattern throughout the cytoplasm, whereas in C2C12 myotubes and some myoblasts, it was localized along stress-fiber-like structures (SFLSs) or immature myofibrils in an intermittent pattern, in addition to its dotted sarcoplasmic distribution (Fig. 4A-F).

The three plectin fragments colocalized at least partly with β-synemin in C2C12 cells (Fig. 4J-X), suggesting their intracellular interactions with β-synemin. Plectin Ex1 fragments were primarily localized in the nucleus and did not colocalize with β-synemin in most of the transfectants (Fig. 4G-I). In some transfectants, however, they were weakly distributed throughout cytoplasm with faint staining of their colocalization with β-synemin (Fig. 4J-L). These results could be interpreted as follows: overexpression of Ex1 fragments resulted in their distribution at the cytoplasm, where they were preferentially distributed along β-synemin-associated SFLSs, although the fragments were mostly localized in the nucleus because of a putative nuclear localization signal included in them (Rezniczek et al., 2003). Plectin CHDα fragments appeared to colocalize with β-synemin along SFLS and in the sarcoplasm, where they were distributed in a pattern somewhat more patchy than a dotted pattern of β-synemin (Fig. 4M-R). Plectin PlD-M fragments were locally distributed in an irregularly intermittent pattern along a subset and some parts of β-synemin-associated SFLSs, and almost lack their sarcoplasmic distribution, indicating their partial colocalization with β-synemin along some portions of SFLSs (Fig. 4S-X).

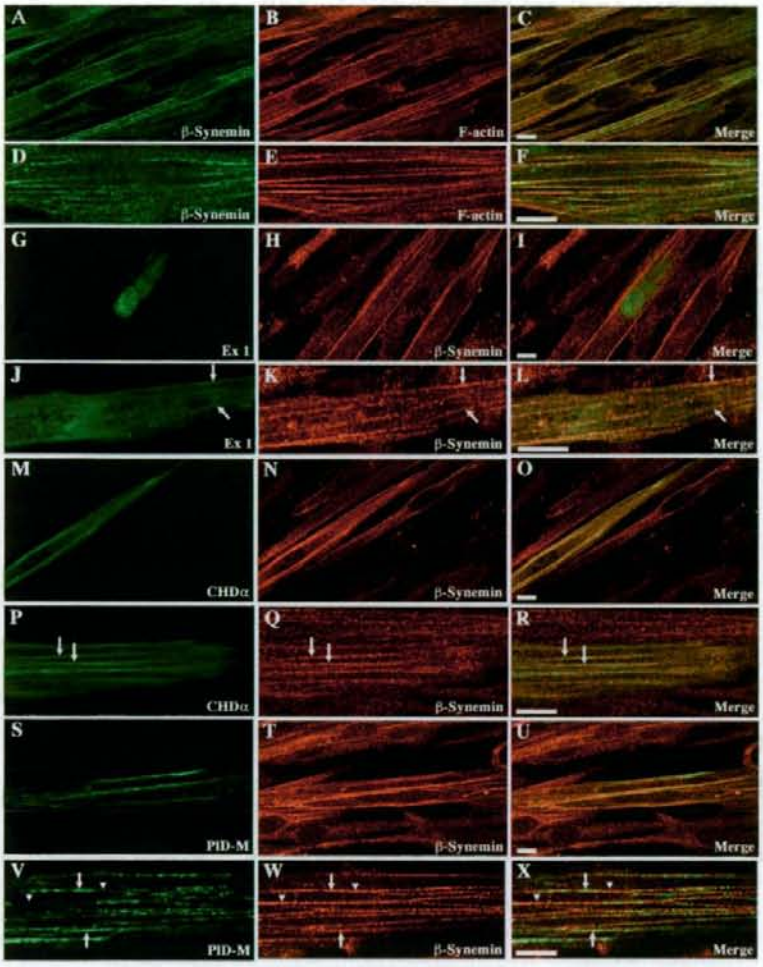

Fig. 4. Subcellular localization of mutant plectin fragments containing a β-synemin-binding site in transfected C2C12 myoblasts and myotubes. C2C12 myoblasts were transfected with plasmids expressing Myc-tagged plectin Ex 1, CHDα and PlD-M fragments, and then cultured in differentiation medium. At 60-84 hours post transfection, differentiated myotubes were immunolabeled with antibodies specific for Myc and β-synemin. Localization of β-synemin along SFLSs and throughout the sarcoplasm in a dotted pattern was found in control myotubes doubly immunolabeled with Alxea-Fluor-594-conjugated phallotoxins and anti-β-synemin pAb (A-F). The three mutant plectin fragments more or less colocalized with β-synemin along SFLS (arrows in J-L,P-R,V-X). Arrowheads in V and X indicate sites associated predominantly with β-synemin, but scarcely with PlD-M. Bars, 10 μm.

In vitro interactions of plectin 1 and β-synemin with F-actin

The present pull-down assay showed that plectin CHDα, including actin-binding sites, interacted with β-synemin tail fragments (Tail N1). This prompted us to examine the effect of β-synemin Tail N1 on the actin-binding of plectin CHDα. First, we confirmed in vitro interaction of plectin CHDα with F-actin. Consistent with previous reports (Fontao et al., 2001; Geerts et al., 1999), plectin CHDα co-sedimented with F-actin, whereas it was found in the soluble fraction in the absence of F-actin (Fig. 5, lanes 2 and 3). Next, we tested in vitro interaction of β-synemin Tail N1 with F-actin. Unexpectedly, β-synemin Tail N1 fragments slightly co-sedimented with F-actin, but were hardly found in the pellet fraction in the absence of F-actin (Fig. 5, lanes 4-6). These results indicated a direct, but weak association of β-synemin tail fragments with F-actin. In a co-sedimentation assay to assess the effect of β-synemin Tail N1, F-actin was polymerized in the presence of plectin CHDα, incubated with a tenfold molar excess of β-synemin Tail N1, and then sedimented by centrifugation. Even in the presence of β-synemin Tail N1, plectin CHDα was found to be associated with F-actin and almost absent in the soluble fraction (Fig. 5, lanes 7 and 8). These results indicated that β-synemin Tail N1 did not inhibit interactions of plectin CHDα with F-actin under this experimental condition.

In vitro interactions of plectin 1 with β-synemin and α-dystrobrevin

The present pull-down assays demonstrated that plectin 1 bound the rod domain 2B and N-terminal tail domain of β-synemin, whereas a previous study reported that α-dystrobrevin interacted with the β-synemin rod domain (Mizuno et al., 2001). These findings implied that plectin 1 and α-dystrobrevin compete with each other for β-synemin owing to the partial overlap of their interacting sites on the rod domain – although we initially presumed that plectin 1 interacted with β-synemin, which in turn bound

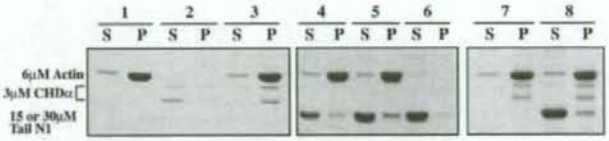

Fig. 5. In vitro interactions of plectin 1 and β-synemin with F-actin. Bindings of plectin CHDα and β-synemin Tail N1 fragments to F-actin were demonstrated by actin co-sedimentation assay. After centrifugation, most of CHDα fragments (3 μM) were found in the pellet (P) in the presence of F-actin (6 μM), whereas they remained in the supernatant (S) in the absence of actin (lanes 2 and 3). Small amounts of β-synemin Tail N1 fragments were sedimented in the presence of F-actin (15 μM and 30 μM β-synemin in lanes 4 and 5, respectively), while in the absence of F-actin, the Tail N1 fragments (30 μM) were observed mostly in the supernatant (lanes 6). Even in the presence of a 10-fold molar excess of Tail N1 fragments (30 μM), CHDα fragments were still found mostly in the pellet together with F-actin (compare lanes 7 with lanes 8).

α-dystrobrevin. This presumptive molecular array of plectin 1, β-synemin and α-dystrobrevin was examined in immunoprecipitation experiments using Myc-tagged PleN1 fragments, GST-fused full-length β-synemin and α-dystrobrevin fragments including products of exons 8 to 16, which were indispensable for interactions with β-synemin (Mizuno et al., 2001). Prior to this experiment, interactions of β-synemin with α-dystrobrevin were ascertained by pull-down assay. Using glutathione beads, GST-fused β-synemin pulled down α-dystrobrevin fragments, whereas GST protein alone did not (Fig. 6A). Next, interactions of plectin 1 with α-dystrobrevin were also tested by immunoprecipitation. In this experiment, Myc-tagged LacZ recombinant proteins and N-terminal fragments of plectin 1f (PleN1f) were used as control and comparison samples, respectively. Plectin 1f is an alternative variant differing from plectin 1 only in the first exon and is most likely to interact with α-dystrobrevin, because it is preferentially distributed along the sarcolemma of skeletal muscle fibers (Rezniczek et al., 2007). In contrast to this prediction, only PleN1 coimmunoprecipitated with α-dystrobrevin fragments, whereas neither PleN1f nor LacZ did (Fig. 6B). These results indicated that plectin 1 directly interacts with α-dystrobrevin through its unique exon 1 part.

To assess the formation of the presumptive molecular array, full-length β-synemin, α-dystrobrevin fragments and Myc-tagged PleN1, PleN1f or LacZ were incubated and then coimmunoprecipitated using anti-Myc antibody and protein L-agarose beads. As shown in Fig. 6C, PleN1 fragments coimmunoprecipitated with α-dystrobrevin fragments as well as β-synemin, whereas PleN1f fragments coimmunoprecipitated with β-synemin but not α-dystrobrevin fragments. Taking account of β-synemin- and α-dystrobrevin-binding sites on plectin 1 and plectin 1f, these results suggest that plectin 1 and plectin 1f can bind β-synemin at their CH and/or plakin domains, thereby probably preventing the association of β-synemin with α-dystrobrevin, whereas plectin 1 can interact further with α-dystrobrevin or both α-dystrobrevin and β-synemin through its exon 1 part. In control experiments, neither LacZ fragments nor PleN1 in combination with control IgG significantly precipitated α-dystrobrevin and β-synemin.

In vitro interactions of plectin 1 with α-dystrobrevin, F-actin and β-synemin

The results presented so far indicate that plectin PleN1 fragments can interact with α-dystrobrevin, F-actin and β-synemin. To assess whether plectin 1 forms a molecular complex with all of these three proteins, we performed a blot overlay assay. PleN1 fragments were immobilized on nitrocellulose membrane, overlaid and incubated with one of the three proteins or the mixture of all the proteins, followed by detection of bound proteins using antibody specific for each protein. As shown in Fig. 7, comparison of resulting signals indicated no significant differences between overlays of each protein alone and of the three proteins. These results suggest a possibility that plectin 1 can form molecular complexes with all of α-dystrobrevin, F-actin and β-synemin.

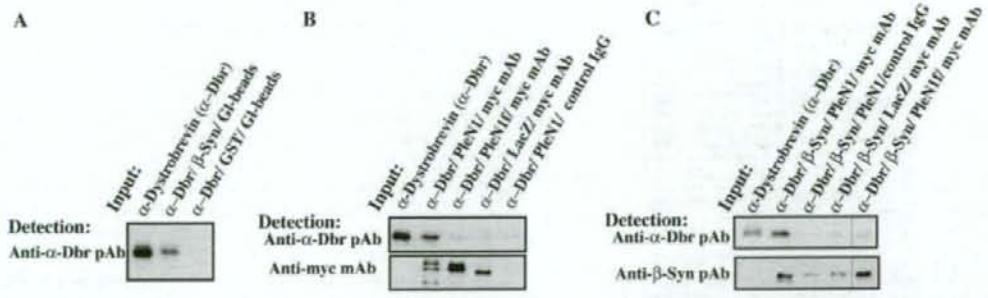

Fig. 6. In vitro interactions of plectin 1 with α-dystrobrevin and β-synemin. (A) α-Dystrobrevin fragments (α-Dbr, 0.8 μg) were incubated with GST-fused β-synemin (β-Syn, 10 μg) or GST (1.8 μg) in the incubation buffer (1 ml) and then precipitated by glutathione beads (Gl-beads, 50 μl). GST-fused β-Syn precipitated α-Dbr, but GST alone did not. (B) α-Dbr (0.5 μg) were incubated with Myc-tagged plectin 1 (PleN1, 9.6 μg) or plectin 1f fragments (PleN1f, 3.2 μg) or β-galactosidase (LacZ, 7.6 μg) in the incubation buffer (1.4 ml) including 0.4% BSA and then immunoprecipitated with anti-Myc antibody (4 μg) and protein L-agarose (40 μl). PleN1 coimmunoprecipitated with α-Dbr, but neither PleN1f nor LacZ did. (C) α-Dbr (0.4 μg) and GST-fused β-Syn (2 μg) were incubated with Myc-tagged PleN1 (9 μg) or PleN1f (3 μg) or LacZ (9 μg) in the incubation buffer (1.2 ml) including 0.4% BSA and then immunoprecipitated with anti-Myc antibody (4 μg) and protein L-agarose (40 μl). PleN1 coimmunoprecipitated with both β-Syn and α-Dbr, whereas PleN1f pulled down only β-Syn. However, LacZ and PleN1 in combination with control IgG pulled down none of them.

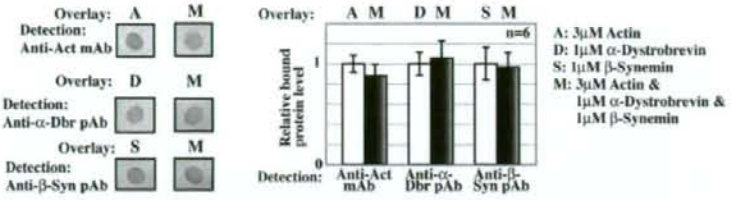

Fig. 7. The assessment of the formation of plectin 1 complexes with F-actin, α-dystrobrevin and β-synemin by blot overlay assays. PleN1 fragments (1 μg) immobilized on nitrocellulose were incubated with 3 μM F-actin (A) or 1 μM α-dystrobrevin fragments (D) or 1 μM GST-fused full-length β-synemin (S) or the mixture of the three proteins (M), followed by detection of bound proteins using antibody specific for each protein. The signals resulting from the overlay with the three proteins were almost equivalent to those from the overlay with each protein alone. Values represent the mean ± s.d. (error bars) of two spots in three independent experiments.

In vivo association of β-synemin and plectin with costameric and cytoskeletal proteins

To explore in vivo association of β-synemin and plectin with costameric components including DGC and cytoskeletal proteins, β-synemin and plectin immune complexes were immunoprecipitated from lysates of muscle LM by anti-β-synemin and anti-plectin antibodies. Subsequently, the presence or absence of proteins in the immune complexes was determined by immunoblotting using antibodies against α-dystrobrevin, dystrophin, pan-actin, (meta)vinculin, desmin and α-actinin. All of the proteins examined, with the exception of α-actinin, were detected in both β-synemin and plectin immune complexes, but control IgG immune complex did not significantly contain any of these proteins (Fig. 8). Desmin coimmunoprecipitated more abundantly with β-synemin than plectin, whereas other proteins, such as dystrophin, metavinculin, α-dystrobrevin 1, α-dystrobrevin 2 and actin, coimmunoprecipitated in greater amounts with plectin. As reported previously (Hijikata et al., 2003), metavinculin, rather than vinculin, was preferentially immunoprecipitated by either of the antibodies.

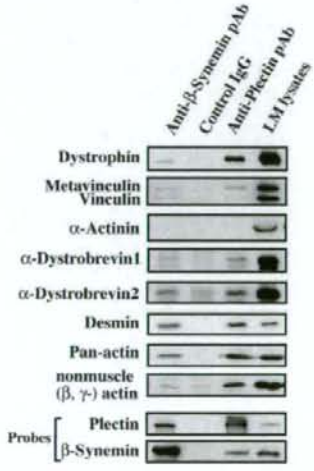

Fig. 8. In vivo interactions of plectin and β-synemin with costameric proteins including DGC. Plectin- and β-synemin-immune complexes were immunoprecipitated from LM lysates by anti-plectin or anti-β-synemin antibodies, respectively. Both the immune complexes contained dystrophin, α-dystrobrevin 1 and α-dystrobrevin 2, meta-vinculin, desmin and actin, including nonmuscle actin, but not α-actinin. In control experiments, control IgG did not significantly coimmunoprecipitate with any proteins.

Next, anti-nonmuscle actin (β- and γ-actin) antibody was used to determine whether costameric nonmuscle actin is associated with β-synemin and plectin in the immune complexes. Both the immune complexes included nonmuscle actin, but its levels were higher in plectin immune complexes. These results suggest that nonmuscle actin, possibly costameric γ-actin, is involved in the interactions of β-synemin and plectin with DGC and other costameric components beneath the sarcolemma. In fact, γ-actin was found to localize predominantly to the costameric sarcolemma, where it seemed to be associated with DGC through dystrophin (Rybakova et al., 2000).

Expression and distribution of IF, IF-associated and DGC proteins in animal models of dystrophin-deficient muscular dystrophy

Since plectin and β-synemin indirectly interacted with dystrophin through α-dystrobrevin, as described above, we postulated that their expression and/or distribution might be affected by the deficiency of dystrophin. Therefore, the expression and distribution of plectin and β-synemin in dystrophin-deficient skeletal muscles were explored by immunoblotting and immunohistochemistry, and compared with those in control muscles. In addition, those of other costameric proteins including α-dystrobrevin were also examined. The specimens were obtained from anterior tibial muscles of wild-type mice and dogs, and dystrophin-deficient X-chromosome-linked muscular dystrophy (mdx) mice and canine X-chromosome-linked muscular dytstrophy in Japan (CXMDJ) dogs.

The expression levels of plectin and β-synemin were significantly elevated in CXMDJ dogs relative to wild-type dogs, whereas they were almost equivalent between wild-type and mdx mice (Fig. 9). For utrophin, integrinβ1d and metavinculin, their expressions were increased in mdx mice and CXMDJ dogs as compared with wild-type controls. However, statistically significant differences were found only between CXMDJ and wild-type dogs, but not between mdx and control mice. The expression levels of vimentin showed a significant increase in mdx and CXMDJ as compared with wild-type controls, whereas those of α-dystrobrevin 1, α-dystrobrevin 2 and α-dystrobrevin 3 represented a significant decrease in dystrophin-deficient muscles relative to controls. The expression levels of vinculin, desmin and α-actinin were almost equivalent between wild-type and mdx or CXMDJ muscles.

The distributions of plectin and β-synemin were slightly altered in dystrophin-deficient muscles of mdx mice and CXMDJ dogs as compared with normal controls (supplementary material Fig. S2A-F). Dystrophin-deficient muscle fibers showed more intense staining for β-synemin and plectin along the sarcolemma as compared with normal muscles. More conspicuous phenotypic alterations were found

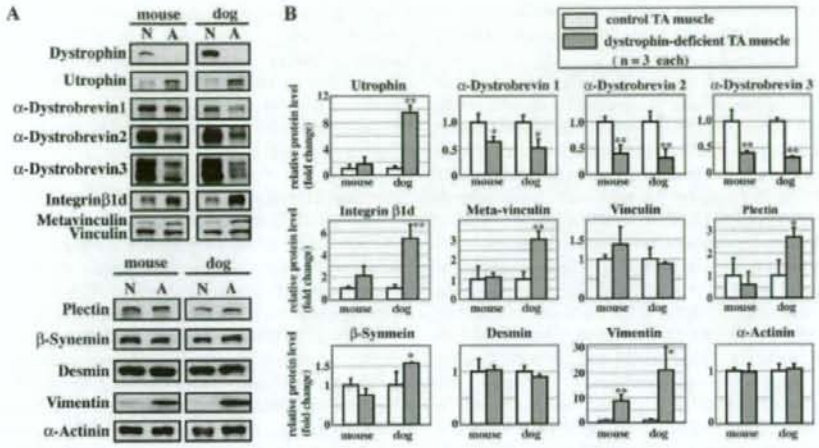

Fig. 9. Immunoblots of costameric, IF-associated and IF proteins from wild-type (N) and dystrophin-deficient (A) mdx mice (5-6 weeks old) and CXMDJ dogs (6-10 months old). (A,B) Reduced expression of α-dystrobrevin 1, α-dystrobrevin 2 and α-dystrobrevin 3, and increased expression of utrophin, integrin β1d, metavinculin and vimentin were detected in dystrophin-deficient mice and dogs when compared with wild-type controls. Note slightly elevated expression of plectin and β-synemin in dystrophin-deficient dogs. Values represent the mean ± s.d. (error bars) of muscle specimens obtained from three mice and dogs. $^{**}P<0.01$ and $^{*}P<0.05$, compared with control mice or dogs.

in IF networks of CXMDJ dogs, but not in those of mdx mice. Aberrant IF networks and/or abnormal sarcoplasmic deposits or aggregates were observed in CXMDJ muscle fibers. Aberrant IF networks appeared as larger and more irregular honeycomb structures when compared with normal controls. The sarcoplasmic deposits were positive for β-synemin, plectin, vimentin and desmin, but negative for utrophin, α-dystrobrevin and integrin β1d. These aberrant IF networks and sarcoplasmic deposits were found mainly in regenerating fibers that were positive for vimentin or developmental myosin staining (supplementary material Fig. S2G-I).

Discussion

It has been long assumed that desmin IFs anchor onto the costameric sarcolemma. Consistent with this assumption, our previous immuno-EM study ultrastructurally demonstrated that plectin linked desmin IFs to dystrophin- and vinculin-containing subsarcolemmal dense plaques, or costameres (Hijikata et al., 2003). Except for plectin, however, proteins involved in the linkages from IF to costameres and their molecular organization remained largely unknown. Recently, direct association of plectin 1f to dystrophin and β-dystroglycan was shown as a linkage between IFs and DGC (Rezniczek et al., 2007). Extending this knowledge further, this study provides new insights into the molecular organization from IF to costameres, by demonstrating that plectin 1 can bind actin, α-dystrobrevin and β-synemin, whereas β-synemin can also bind actin as well as α-dystrobrevin.

β-synemin is a peculiar IF protein involved in molecular organization of actin-based costameres

Unlike other IF proteins, β-synemin can bind actin and actin-associated proteins. These abilities are supported by several lines of evidence, provided by our results and those of others: (1) β-synemin tail fragments slightly co-sedimented with F-actin in the actin co-sedimentation assay; (2) β-synemin was found along SFLS, including actin, in C2C12 myotubes; (3) β-synemin coimmunoprecipitated with sarcomeric and nonmuscle actin from muscle LM lysates; (4) previous yeast-two-hybrid analyses using avian synemin cDNA as a bait demonstrated direct interactions of synemin with α-actinin and vinculin (Bellin et al., 1999; Bellin et al., 2001). However, mammalian β-synemin is unlikely to interact with α-actinin, although it seems to bind vinculin. In the present immunoprecipitation experiment, β-synemin immuno-complexes from LM lysates contained metavinculin but not α-actinin. This absence of β-synemin-interaction with α-actinin was possibly due to the lack of the approximately 300-residue-long C-terminal sequences of avian synemin that are required for binding α-actinin in rat β-synemin molecules.

In costameres, β-synemin seems to serve as an actin-associated protein rather than an IF protein to form heteropolymeric IFs, and is unlikely to link IFs to costameric components. As demonstrated by our immuno-EM analysis, β-synemin appeared to be incorporated into costameric dense plaques without associating with IF. Similar β-synemin-association with the sarcolemma, independent of IF, was found in muscle fibers of desmin knockout mice that lacked desmin IFs (Carlsson et al., 2000). Such β-synemin-associations with the sarcolemma possibly occur through its interactions with α-dystrobrevin, actin, and/or metavinculin within costameres, where β-synemin might contribute to the integration of actin-based molecular architectures. However, β-synemin molecules were incorporated into heteropolymeric IFs as well. These β-synemin molecules, which are heteropolymerized with desmin, would not interact with α-dystrobrevin or dystrophin anymore and, therefore would not link IFs to costameres, because desmin, α-dystrobrevin and dystrophin confine their binding sites onto β-synemin rod domain (Bhosle et al., 2006; Mizuno et al., 2001). This notion is supported by the present immunoprecipitation results, indicating that β-synemin associated with plectin 1f through a part of rod domain could not further co-precipitate with α-dystrobrevin.

Plectin 1, an isoform expressed in skeletal muscle, binds α-dystrobrevin, possibly contributing to its differential targeting to the sarcolemma

Four plectin isoforms (plectin 1, plectin 1b, plectin 1d and plectin 1f) generated by alternative splicing are predominantly expressed in skeletal muscles (Fuchs et al., 1999). They differ from each other only in their small N-terminal sequences that are encoded by their own first exon (exon 1, exon 1b, exon 1d and exon 1f, respectively). A recent study using isoform-specific antibodies and isoform-expression constructs revealed the differential targeting of plectin isoforms in skeletal muscle fibers or myotubes (Rezniczek et al., 2007). Plectin 1 and 1f are preferentially associated with the sarcolemma, whereas plectin 1d is localized exclusively to Z-discs. The differential targeting of plectin 1 to the sarcolemma could be explained by the present finding that its exon 1 part bound α-dystrobrevin. This binding property would target plectin 1 to the sarcolemma associated with α-dystrobrevin. However, the differential localization of plectin 1f at the sarcolemma cannot be explained, because nothing is known of proteins specifically interacting with its exon 1f part. As presented here, plectin 1f fragments did not interact with α-dystrobrevin. Nevertheless, their unique exon 1f parts may interact with other costameric proteins or different domains of α-dystrobrevin, e.g. its exon parts 1 to 7, ultimately leading to its localization at the sarcolemma.

A versatile binding property of the N-terminal part of plectin

At its N-terminus, plectin possesses multifunctional CH domains to interact with multiple proteins, in addition to the plakin domains. The CH domains contain binding sites for actin (Andra et al., 1998), integrin β4 (Geerts et al., 1999; Rezniczek et al., 1998), vimentin (Sevcík et al., 2004), nesprin-3 (Wilhelmsen et al., 2005), the nonreceptor tyrosine kinase Fer (Lunter and Wiche, 2002), dystrophin and utrophin (Rezniczek et al., 2007), whereas the plakin domain was found to bind β-dystroglycan (Rezniczek et al., 2007). The present study has added β-synemin to the lists of CH-domain-binding or plakin-domain-binding proteins. Moreover, an isoform-specific binding site was disclosed in plectin 1, which has unique exon 1 part to bind β-synemin and α-dystrobrevin. These accumulating data underline a versatile binding property of N-terminal parts of plectin. However, this versatile binding property raises questions of how plectin selectively determines and regulates interactions with binding partners.

A model of molecular organization from IF to costameres including DGC and integrin complexes

A model of molecular organization from IF to costameres including DGC and integrin complexes is proposed based on the results of the present and previous studies (Fig. 10A). Plectin 1 interacts with heteropolymeric IFs including desmin and β-synemin through its C-terminal IF-binding domain (Hijikata et al., 2003; Reipert et al., 1999), whereas its N-terminal part binds α-dystrobrevin, costameric actin and β-synemin. The costameric actin bound by plectin 1 might be associated with dystrophin and (meta)vinculin (Rybakova et al., 2000; Witt et al., 2004), whereas β-synemin on plectin 1 molecules might interact further with costameric actin. Moreover, α-dystrobrevin associated with plectin 1 might also bind β-synemin. In addition to this model, another one has been recently proposed (see Fig. 10B), in which plectin 1f links IFs directly to dystrophin and β-dystroglycan within DGC (Rezniczek et al., 2007). This direct binding of plectin to and its indirect interactions through actin with dystrophin well agreed with our previous findings that treatment of plectin immune complexes from LM lysates with gelsolin decreased dystrophin within the immune complexes, but did not completely remove it (Hijikata et al., 2003).

Costameres are structurally and functionally analogous to hemidesmosomes

With respect to linking IFs to the BM, costameres in skeletal muscles are quite analogous to hemidesmosomes in epidermal cells, although costameric components are much more numerous and organized in

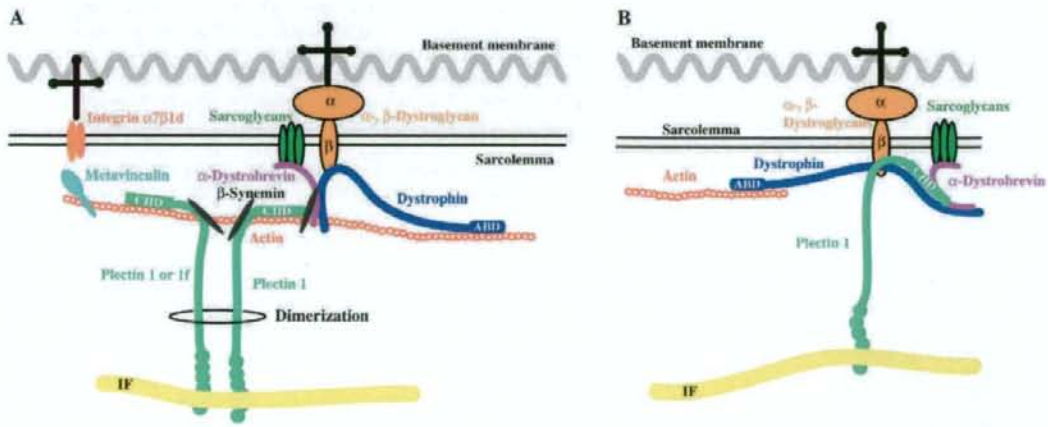

Fig. 10. Models of molecular organization from IF to costameres including DGC and integrin complexes. (A) The N-terminal part of plectin 1 is associated with costameres by binding β-synemin, costameric actin and α-dystrobrevin, whereas its C-terminal part is linking to IFs. Exon 1 part of plectin 1 might interact with not only α-dystrobrevin but also β-synemin, whereas β-synemin on plectin molecules might be further associated with costameric actin linking to plectin, dystrophin and metavinculin. (B) As an alternative model, direct interactions of plectin with dystrophin and β-dystroglycan were proposed by Rezniczek et al. (Rezniczek et al., 2007). This model is partly modified to represent the interaction of plectin 1 with α-dystrobrevin through its exon 1 part.

more complicated manner than hemidesmosomal ones. Costameres including DGC and integrin complexes are extracellularly associated with the BM through α-dystroglycan and integrin α7β1d (Belkin et al., 1996; Eravsti and Campbell, 1993), whereas they are intracelluarly linked to IFs by plectin (Hijikata et al., 2003; Rezniczek et al., 2007; Schröder et al., 2002). Both the analogous structures are assumed mechanically to stabilize the plasma membrane and to protect cell against mechanical stress. Attesting this assumption, similar disruptions of plasma membranes and cell structures were reported to occur in skin or skeletal muscle by the deficiency or defects of constituents of hemidesmosomes or costameres, such as plectin (Andra et al., 1997; Gache et al., 1996; McMillan et al., 2007), IF proteins (desmin and keratin) (Chan et al., 1994; Li et al., 1997) and other membranous or membrane-associated proteins (integrin α7, dystrophin, α-dystrobrevin, sarcoglycan, integrin α6, integrin β4, BP180) (Dowling et al., 1996; Duclos et al., 1998; Grady et al., 1999; Hack et al., 1998; Hoffman et al., 1987; Huber et al., 2002; Mayer et al., 1997; Pulkinnen et al., 1997; van der Neut et al., 1996).

Quantitative alterations of costameric components in dystrophin-deficient muscles

Quantitative alterations of costameric components were found in dystrophin-deficient muscles. In contrast to the reduction of DGC components (Ozawa, 2006; Straub and Campbell, 1997), other costameric components, such as plectin, β-synemin, (meta)vinculin, talin and integrins, increase their expressions in dystrophin-deficient muscles, as demonstrated in the present and previous studies (Hodges et al., 1997; Law et al., 1994; Rezniczek et al., 2007). Increased synemin- and plectin-staining along the dystrophin-deficient sarcolemma were also noted by the present and previous immunohistochemical studies (Schröder et al., 1997). Moreover, costameric γ-actin is also more abundantly expressed in mdx muscles lacking dystrophin, compared with control muscles (Hanft et al., 2006). These increased expressions of costameric components, including integrin complexes, might be a compensatory or an adaptive cellular response to unstable costameres and unstable anchorages of IF on costameres.

As a compensatory response in dystrophin-deficient muscles, increased β-synemin and plectin 1, together with costameric γ-actin, might preserve the subsarcolemmal localization of α-dystrobrevin, which loses a main binding partner dystrophin beneath the sarcolemma. As presented in this study, β-synemin and plectin 1 can bind α-dystrobrevin. Another possibility is that sarcoglycan-sarcospan complex also contributes to recruitment of α-dystrobrevin to the sarcolemma, because the complex interacts with the N-terminal portion of α-dystrobrevin and is still present in the dystrophin-deficient sarcolemma (Hack et al., 2000; Ozawa et al., 2000; Yoshida et al., 2000). In this context, it is worth noting that utrophin, a structurally related protein that can compensate for lack of dystrophin, might not retain α-dystrobrevin at the sarcolemma. α-Dystrobrevin 2 localized at the extrasynaptic sarcolemma was found not to interact with utrophin (Peters et al., 1998).

Functional significances of costameres connecting to IF through plectin

DGC and integrin complexes within costameres would have the similar function of linking the BM to IFs through plectin, costameric actin and β-synemin. This would result in stabilizing the sarcolemma and protecting it against contraction-imposed stress. Their functional similarity would be reasonably supposed, given that the reduction of DGC induced a compensatory response of increased expression of integrin complexes. However, the two complexes would also have their own functional roles, because dystrophin-deficient muscles still undergo degeneration despite increased expression of integrin complexes. This fact implies that increased integrin complexes are not sufficient, either quantitatively or qualitatively, to compensate for functional roles of DGC. The two complexes in combination with plectin and IFs might serve as platforms for distinct signal transduction, because DGC and integrin complexes are associated with distinct proteins involved in different signaling, i.e. nNOS and FAK, respectively (Brenman et al., 1996; Pharn et al., 2000).

Materials and Methods

Cloning of rat β-synemin, plectin isoforms and α-dystrobrevin cDNA

To clone cDNA of a plectin-binding protein, a rat skeletal muscle 5′-stretch plus cDNA library (Clontech) was screened with DNA probes, which were prepared by PCR using the cDNA library and a pair of primers predicted from partial amino acid sequences (5′-CCNCAYGARTTYCAY-3′ for PHEFH and 5′-RTCNACCATYCT-YTG-3′ for QRMVD). This screening identified 47 positive clones that did not contain a 5′ sequence with an ATG start codon. Therefore, to clone the full-length cDNA, we constructed a cDNA library from single-stranded DNAs generated by reverse transcription using mRNA obtained from skeletal muscles of newborn rats, random hexamers and gene-specific primers based on the sequences of incomplete cDNAs (5′-CATGCGCTCAGGCAACGTTTCCTCCAGCTG-3′ and 5′-TTGACTCTGT-CTGGTCAGGGCAGACAGCTG-3′). This cDNA library was screened with a new probe that had been generated from a positive cDNA clone obtained in the previous screening to identify ten overlapping cDNA clones including the full-length clone.

To obtain cDNA clones encoding the N-terminal parts of various plectin isoforms (exon 1–exon 30), a partial cDNA library was constructed (as described above) with random hexamers, and rat plectin-specific primers (5′-TTCATCCAGAGCC-TGCAGGCCCGCTGCTT-3′, 5′-TCTCTGCCTCGGCTTGGCACAGCCACCGTT-3′, and 5′-TTCTCCAGCTCCTGCTCAGCCAGCTCTCGC-3′). This library was screened with DNA probes generated using rat plectin cDNA fragments (plectin 1, 1-1311bp), which were obtained by RT-PCR using total RNA of new-born rat skeletal muscles and a pair of rat plectin 1-specific primers (5′-ATGGTGGCTGG-CATGCTCATG-3′ and 5′-GTGGTGCCGGATCCACTHTAG-3′). Thirty-three positive clones were identified and found to include various plectin isoforms, such as plectin 1, 1a, 1b, 1d, 1f and 1e.

α-Dystrobrevin cDNA encoding exon 8 to exon 16 was amplified from the rat skeletal muscle 5′-stretch plus cDNA library by PCR using a pair of primers (5′-GCNAAYGTNGARAAYGTNTTYCAYCCNGTNG-3′ and 5′-RTAYTCYTCCAT-YTGNAGYTCRTTYTCNAG-3′). These primers were designed based on the published sequences of mouse and human α-dystrobrevin 1. A cDNA of approximately 1.5 kb was obtained and sequenced to confirm that it was an α-dystrobrevin cDNA fragment encoding amino acid residues 232-669 of α-dystrobrevin isoform1 isoform11 (XP_001054793).

Expression and purification of GST or 6xHis recombinant proteins

β-Synemin constructs encoding the following segments of the protein were subcloned into pGEX-6p-1 glutathione S-transferase (GST) bacterial expression vector (GE Healthcare): full-length (amino acids 1-1255), Rod N (1-130), Rod MI (56-286), Rod Ms (57-223), Rod C (169-318), Tail N1 (303-578), Tail N2 (303-432), Tail M (482-930), Tail C1 (822-1255), Tail C2 (931-1102), and Tail C3 (1071-1255). Similarly, cDNA fragments encoding full-length β-galactosidase (LacZ), the N-terminal portion of plectin 1 including exon 1 (PleN1, amino acids 1-1273), the N-terminal part of plectin 1f including exon 1f (PleN1f, 1-1121), exon 1 (Ex1, 1-181), calponin homology domain (CHDα, 183-507), various plakin domain fragments (PlD-N, 413-736; PlD-MC, 707-1273; PlD-M, 707-950; PlD-Cl, 854-1273; PlD-Cs, 965-1273) were subcloned into the pGEX-6p-1. All of these plectin fragments and β-galactosidase contained the Myc-tag epitope at their C-termini. α-Dystrobrevin cDNA fragment obtained from the rat skeletal muscle cDNA library was subcloned into the pET-19b vector carrying an N-terminal 6xHis tag sequence (Novagen). Escherichia coli BL21 (DE3) was transformed with the constructs described above. Expression of GST or 6xHis fusion proteins was induced by 0.2 mM IPTG for 3 h at 28°C. Purification of GST or 6xHis fusion proteins was performed as described in the respective manufacturer's protocols. GST was removed from plectin recombinant fragments and LacZ by digestion with PreScission protease (GE Healthcare) on glutathione bead columns.

Antibodies

Rabbit β-synemin antisera were raised against recombinant rat synemin tail fragments (amino acids 822-1255). The antisera were purified by passage over affinity columns